© 2018. Published by The Company of Biologists Ltd | Development (2018) 145, dev159368. doi:10.1242/dev.159368

RESEARCH ARTICLE

Notch1 is asymmetrically distributed from the beginning of embryogenesis and controls the ventral center

Aitana M. Castro Colabianchi[1,*], Diego R. Revinski[1,2,*], Paula I. Encinas[1], María Verónica Baez[1], Renato J. Monti[1], Mateo Rodríguez Abinal[1], Laurent Kodjabachian[2], Lucía F. Franchini[3] and Silvia L. López[1,‡]

ABSTRACT

Based on functional evidence, we have previously demonstrated that early ventral Notch1 activity restricts dorsoanterior development in *Xenopus*. We found that Notch1 has ventralizing properties and abolishes the dorsalizing activity of β-catenin by reducing its steady state levels, in a process that does not require β-catenin phosphorylation by glycogen synthase kinase 3β. In the present work, we demonstrate that Notch1 mRNA and protein are enriched in the ventral region from the beginning of embryogenesis in *Xenopus*. This is the earliest sign of ventral development, preceding the localized expression of *wnt8a*, *bmp4* and Ventx genes in the ventral center and the dorsal accumulation of nuclear β-catenin. Knockdown experiments indicate that Notch1 is necessary for the normal expression of genes essential for ventral-posterior development. These results indicate that during early embryogenesis ventrally located Notch1 promotes the development of the ventral center. Together with our previous evidence, these results suggest that ventral enrichment of Notch1 underlies the process by which Notch1 participates in restricting nuclear accumulation of β-catenin to the dorsal side.

KEY WORDS: Notch, β-catenin, Dorsoventral development, BMP, Wnt8a, Ventx, *Xenopus*, Zebrafish

INTRODUCTION

During the past two decades, many studies, mostly performed in amphibian and fish embryos, have demonstrated that an antagonistic interplay between two signaling centers, a ventral center (VC) and a dorsal center (the gastrula Spemann–Mangold's organizer, SMO), pattern the dorsoventral (DV) and anteroposterior body axes in vertebrates. The VC, which has been described at the gastrula stage, secretes BMP4 and Wnt8a (De Robertis, 2009; Thisse and Thisse, 2015). These morphogens induce ventral-posterior fates in the embryo, whereas the dorsal center secretes antagonists and expresses transcriptional repressors of the ventral morphogens, thus protecting the dorsal region from their ventralizing and posteriorizing activities (De Robertis, 2009; Thisse and Thisse, 2015). The SMO derives from the 'blastula chordin- and noggin-expressing center' (BCNE), which appears when zygotic transcription begins. The BCNE secretes the BMP antagonists that confer its name, and also contains the precursors of the brain. Its formation is triggered by a Wnt/β-catenin cascade activated as a consequence of the relocation of dorsal determinants after fertilization (Kuroda et al., 2004). β-Catenin accumulates in dorsal nuclei and activates the transcription of Siamois-related homeobox (Sia) genes. These homeodomain proteins are the first transcription factors expressed in the BCNE and, in turn, both repress (probably indirectly) *bmp4* transcription and transiently activate the expression of the BMP antagonists in the prospective anterior neuroectoderm. This double inhibition of BMP signaling, which is initiated at blastula stages, is crucial for brain formation (Wessely et al., 2001; Kuroda et al., 2004; De Robertis and Kuroda, 2004; Ishibashi et al., 2008). Importantly, whether an event of asymmetric distribution of ventral determinants analogous to that triggered by Wnt dorsal signaling occurs in the earliest stages of embryogenesis has not yet been determined, as molecules involved in ventral development have not shown evidence of an early uneven allocation in the initial DV axis (see below).

Knockdown experiments have demonstrated that the most important BMP signals for ventral development are BMP4 and BMP7 (Reversade et al., 2005). In *Xenopus*, *bmp7.2* transcripts (but not *bmp4* transcripts, which begin to accumulate during gastrulation) are stored to a significant level in eggs (Nishimatsu et al., 1992; Session et al., 2016). During early cleavage stages, *bmp7.2* mRNA is ubiquitously distributed in the animal hemisphere, and zygotic *bmp4* and *bmp7.2* mRNAs show a uniform expression in ectoderm and mesoderm in late blastulae. During gastrulation, *bmp4* and *bmp7.1* transcripts accumulate at high levels in the VC, and *bmp7.2* mRNA retains a uniform distribution in the entire mesoderm (Hemmati-Brivanlou and Thomsen, 1995; Hawley et al., 1995; Kirmizitas et al., 2017). BMPs act by activating the expression of the Ventx family of ventral transcriptional repressors (Gawantka et al., 1995; Onichtchouk et al., 1996; Shapira et al., 1999; Rastegar et al., 1999; Henningfeld et al., 2000). The BMP signaling cascade directly activates *vent-2B* transcription at the promoter level (Henningfeld et al., 2000).

Wnt8a transcripts are not maternally stored in *Xenopus*. They begin to accumulate in the ventral region at late blastula (Session et al., 2016; Smith and Harland, 1991), being detectable by *in situ* hybridization (ISH) earlier than *bmp4*. Overexpression of *wnt8a* after the mid-blastula stage, by injection of plasmid DNA, gives rise to ventralized phenotypes (Christian and Moon, 1993), whereas its knockdown results in dorsalization (Li et al., 2006). It has been suggested that *wnt8a* transcription probably depends on maternal BMP signaling, as a dominant-negative BMP receptor suppressed *wnt8a* expression (Hoppler and Moon, 1998). Both Wnt8a and BMP signaling are cooperatively required for ventrolateral mesoderm development, by

[1]Universidad de Buenos Aires, Consejo Nacional de Investigaciones Científicas y Técnicas, Instituto de Biología Celular y Neurociencias 'Prof. E. De Robertis' (IBCN), Facultad de Medicina. Laboratorio de Embriología Molecular 'Prof. Dr. Andrés E. Carrasco', C1121ABG Buenos Aires, Argentina. [2]Aix Marseille Université, CNRS, IBDM, 13288 Marseille, France. [3]Instituto de Investigaciones en Ingeniería Genética y Biología Molecular (INGEBI), Consejo Nacional de Investigaciones Científicas y Técnicas (CONICET), C1428ADN Buenos Aires, Argentina.
*These authors contributed equally to this work

‡Author for correspondence (slopez@fmed.uba.ar)

A.M.C., 0000-0002-8052-8344; D.R.R., 0000-0001-8584-1340; P.I.E., 0000-0001-8265-921X; M.V.B., 0000-0001-5105-2888; R.J.M., 0000-0001-8433-9113; M.R.A., 0000-0003-3969-6570; L.K., 0000-0002-4000-612X; L.F.F., 0000-0001-6602-2243; S.L.L., 0000-0002-3760-7549

Received 12 September 2017; Accepted 25 May 2018

Development (2018) 145, dev159368. doi:10.1242/dev.159368

promoting the expression of Ventx genes (Hoppler and Moon, 1998). Also, in zebrafish, both Wnt8a and zygotic BMP are necessary for the maintenance of Ventx transcript levels during gastrulation; however, Wnt8a is required earlier for this task, at the blastula/gastrula transition, whereas zygotic BMP is the main positive regulator of Ventx genes at mid- to late gastrula (Ramel and Lekven, 2004). Wnt8a expressed after the mid-blastula transition operates through canonical β-catenin/Tcf signaling by stabilizing cytosolic, free β-catenin, which activates gene expression in a Tcf-dependent fashion, as shown in *Xenopus* (Darken and Wilson, 2001). Moreover, Wnt8a induces transcription of Ventx genes by the canonical β-catenin/Tcf pathway, as shown in zebrafish (Ramel and Lekven, 2004).

Ventx genes start their expression at mid-blastula transition (Session et al., 2016). There are different subclasses of these genes in *Xenopus* (Scerbo et al., 2012). Their transcripts show similar expression patterns, being uniformly expressed in the animal hemisphere of blastulae and later restricted to the VC during gastrulation (Gawantka et al., 1995; Onichtchouk et al., 1996; Rastegar et al., 1999; Shapira et al., 1999; Nordin and LaBonne, 2014). Ventx proteins promote ventralization, and exert their action by directly repressing organizer-specific genes (Gawantka et al., 1995; Onichtchouk et al., 1996, 1998; Shapira et al., 1999, 2000; Sander et al., 2007). It was proposed that the early widespread expression of Ventx repressors establishes an anti-organizer activity throughout the embryo, which is later overcome on the dorsal side because of local activation of Wnt/β-catenin signaling triggered by cortical rotation after fertilization (Shapira et al., 2000). It was also suggested that Ventx proteins protect the prospective ventral region from premature commitment towards dorsal fates rather than directly promoting ventral differentiation (Scerbo et al., 2012).

The transmembrane receptor Notch is involved in multiple developmental programs in metazoans. When the pathway is activated, Notch can stimulate or inhibit cell proliferation, cell death, specific cell fates or differentiation in a context-dependent fashion. In the canonical pathway, the main transcriptional mediator of Notch signaling is known as CSL (from the names in vertebrates, fly and worm: CBF1, Su(H) and Lag1, respectively). The Notch receptor is activated by binding to a DSL ligand (characterized by a Delta/Serrate/LAG-2 motif) present on the surface of a neighboring cell. In the absence of such signaling, a repressor complex containing CSL inhibits the transcription of Notch-target genes. Binding of the DSL ligand to the mature Notch receptor triggers a sequence of proteolytic cleavages (involving the enzyme complex γ-secretase), leading to the release of the Notch intracellular domain (NICD). NICD translocates to the nucleus and binds CSL. The co-repressors bound to CSL are displaced, and co-activators are recruited in a new complex, which activates the transcription of Notch-target genes (Kopan and Ilagan, 2009).

We have previously shown that overexpression of the Notch1 intracellular domain (NICD1) resulted in ventralized phenotypes with a loss of cephalic structures in *Xenopus laevis* (*Xla*) embryos (Acosta et al., 2011). This was accompanied by downregulation of the genes encoding the BMP antagonists Chordin and Xnr3 in the BCNE. Conversely, attenuation of *notch1* with a translational-blocking morpholino (Notch1 Mo) enhanced dorsoanterior development. Strikingly, when we injected $su(H)1^{DBM}$ mRNA to impair the canonical, CSL-dependent Notch pathway, we did not observe an expansion of the *chordin* or *Xnr3* domains on the animal hemisphere at blastula s9. We found that Notch1 restricts the expression of these BMP antagonists to the BCNE center by destabilizing maternal β-catenin rather than by a mechanism that relies on CSL-mediated transcription. Gain of function of Notch1 abolished the dorsalizing activity of β-catenin by reducing its steady state levels before mid-blastula transition, even if the β-catenin protein lacked the glycogen synthase kinase-3β (GSK-3β) phosphorylation sites. Notch1 Mo increased the levels of endogenous β-catenin protein, and those of the β-catenin form resistant to GSK-3β-mediated degradation. Thus, we proposed that Notch1 has ventralizing properties, and that early ventral Notch1 activity contributes to the restriction of the BCNE center to the dorsal side of the blastula. This occurs through a non-canonical mechanism via the destabilization of β-catenin in a process that does not require β-catenin phosphorylation by GSK-3β. Through restricting the extent of the BCNE within the animal hemisphere, Notch1 controls the size and the anteroposterior pattern of the brain (Acosta et al., 2011). This negative regulation of β-catenin by Notch1 strongly resembles that described in the wing imaginal disc in *Drosophila* (Hayward et al., 2005, 2008; Sanders et al., 2009; Muñoz-Descalzo et al., 2010) or in mouse embryonic day 14 embryonic stem cells (ESCs) (Kwon et al., 2011), in which membrane-bound Notch negatively titrates transcriptionally active hypophosphorylated β-catenin through a physical post-translational interaction that leads to its lysosomal degradation without the intervention of the GSK-3β-dependent activity of the β-catenin destruction complex. Notably, Notch1 is the predominant Notch receptor involved in regulating the levels of active β-catenin in ESCs (Kwon et al., 2011).

In the present work, we addressed whether the Notch ventral activity that antagonizes hypophosphorylated β-catenin (Acosta et al., 2011) could be due to an asymmetric distribution of Notch1 protein and/or mRNA, and whether Notch1 is able to control the development of the VC. Through immunodetection studies, we found that Notch1 protein is consistently enriched in the ventral side from the beginning of embryogenesis in *Xla* embryos. ISH and RT-qPCR analysis also showed a ventral enrichment of *notch1* mRNA, suggesting that the asymmetry of the protein might be due to a mechanism that controls mRNA localization. We also observed an asymmetric distribution of Notch1 protein in zebrafish from the beginning of embryogenesis. By the mid-blastula stage, an opposite distribution of Notch1 and nuclear β-catenin in both species is established. To our knowledge, the accumulation of Notch1 mRNA and protein shown here is the earliest localized sign of ventral development reported in vertebrates. By performing gain- and loss-of-function experiments in *Xenopus*, we show that Notch1 is required for the normal expression of genes essential for a wholly functional VC.

RESULTS

Notch1 protein is ventrally located during *Xenopus* and zebrafish early embryogenesis and establishes an opposite distribution in relation to β-catenin

In this work, to study the distribution of Notch1 protein during early embryogenesis, we first performed a whole-mount immunofluorescence (IF) analysis in left and right halves of *Xenopus* embryos collected from Nieuwkoop and Faber stage (s) 1 to s8 and then corroborated the results by IF on cryostat sections. Left and right halves were cut from batches of regularly cleaving embryos in which the paler pigmentation zone was bisected by the first cleavage furrow, as the paler region predicts the prospective dorsal side with 70% accuracy in *Xla* (Klein, 1987). Notably, we found a clear and very consistent asymmetric distribution of Notch1 protein, with the highest levels ventrally and the lower levels dorsally. This was seen in all stages analyzed, in both left and right halves, in cryostat

Development (2018) 145, dev159368. doi:10.1242/dev.159368

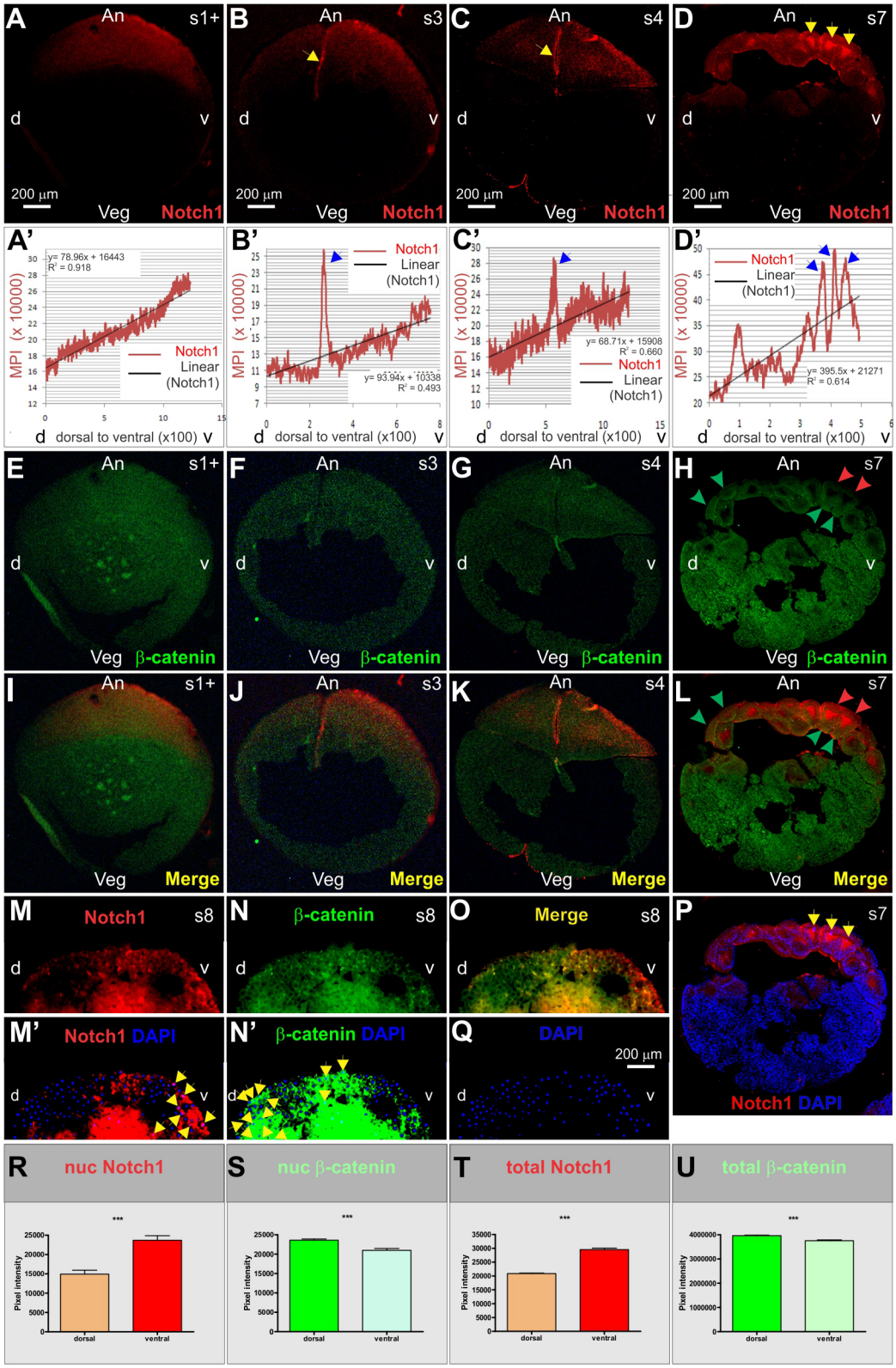

Fig. 1. See next page for legend.

sections (81%, *n*=28) (Fig. 1A-D′,I-M′,P; Table S1) and in whole-mount IF (89%, *n*=136, in a total of six independent batches; Figs S1-S4). Control experiments showed that the primary antibody specifically recognizes Notch1 protein in *Xenopus* embryos (Fig. S5A-F) and that the secondary antibody did not show non-specific fluorescence (Fig. S5G-H′). The ventral enrichment of Notch1 protein was confirmed by western blot (WB) of protein extracts of ventral and dorsal halves obtained at s3 and s7 (Fig. 2A).

To compare the distribution of endogenous Notch1 and β-catenin proteins, we performed whole-mount double IF in left and right

Development (2018) 145, dev159368. doi:10.1242/dev.159368

Fig. 1. Distribution of endogenous Notch1 and β-catenin proteins from s1 to mid-blastula in cryostat sections of *Xenopus* embryos. Left halves of embryos were collected at the indicated stages and were then cut into 20 µm cryostat sections. The embryonic early axes were predicted according to the original pigmentation. (A-D) Notch1 IF was significantly higher in the ventral than in the dorsal region. This was confirmed by comparing vROI with dROI quantifications (P<0.0001, not shown). (A′-D′) Quantification of Notch1 IF of the embryos shown in A-D, respectively. Mean pixel intensity (MPI, *y*-axis) in a rectangular animal ROI was plotted (red line) in relation to the position in the DV axis (*x*-axis). The black line shows a linear estimate by linear regression analysis (parameters shown in inset): a positive slope indicates the increase of Notch1 IF from dorsal to ventral. The yellow arrows in B and C show Notch1 IF in the cell membranes between the animal dorsal and animal ventral blastomeres at s3 and s4, which correlate with the high peaks indicated with the blue arrows in B′ and C′, respectively. Note the ventral nuclei with highest Notch1 signal (D,P, yellow arrows), which correlate with the highest peaks in the profile in this s7 embryo (D′, blue arrows). (E-H) Total β-catenin IF from s1+ to s7. Although the IF in the images was low and noisy at the earliest stages (most evident in F,G), quantification in dROIs and vROIs in E-H (not shown) revealed that it was significantly higher in the ventral region in E (P<0.0001) and in G (P=0.0006), while there was no significant difference between the dorsal and the ventral regions in F (P=0.11). In the embryo shown at s7 (H), total β-catenin IF was significantly higher in the dorsal ROI (P<0.0001). (I-L) Merged images of Notch1 and β-catenin IF. Note the lower total β-catenin IF in the apical region of the ventral cells, which instead show high Notch1 IF (H,L, red arrows). Total β-catenin IF appears higher in the basal region of these cells and more uniform in the dorsal cells (H,L, green arrows) (see Fig. S4 for another example). (M-Q) Notch1 IF (M) and β-catenin IF (N) in an s8 embryo. (M′,N′) Highly contrasted images of M and N, respectively, merged with the DAPI nuclear image (Q) to facilitate visualization of Notch1$^+$ nuclei on the ventral side (M′, yellow arrows) and β-catenin$^+$ nuclei in the dorsal side (N′, yellow arrows). (O) Merged image of M and N, showing highest levels of Notch1 IF in the ventral side and highest levels of total β-catenin IF in the dorsal side in this s8 embryo. (P) Merged DAPI and Notch1 IF of s7 embryo. (R) Notch1 IF in the nuclear region was significantly higher in the ventral side. (S) β-Catenin IF in the nuclear region was significantly higher in the dorsal side. (T,U) Quantification of total Notch1 (T) and total β-catenin (U) in dorsal and ventral ROIs of the images shown in M and N, respectively. The ventral region expresses significantly higher levels of Notch1 protein than the dorsal region; in contrast, the dorsal region expresses significantly higher levels of β-catenin protein than the ventral region. Data are mean+s.e.m. ***P<0.0001 (double-tailed Mann–Whitney test). An, animal; d, dorsal; s, stage; v, ventral; Veg, vegetal.

halves. Analysis by whole-mount IF in three of the previous batches suggested that, at the earliest stages, the highest levels of total β-catenin protein in some embryos were relatively displaced in relation to the region containing the highest levels of Notch1 (for example, compare white and light blue asterisks in Fig. S1B,C,F,G and in Fig. S2B-D; white asterisks and light blue arrows in Fig. S2F-H,N-P; Table S2). In thin cryostat sections, β-catenin IF was low and noisy at the earliest stages analyzed. We were unable to detect a consistent biased distribution for total β-catenin in the DV axis at early cleavage stages (Fig. 1E-L, Table S1). Cryostat sections of s7 embryos confirmed the ventral enrichment of Notch1 protein (Fig. 1D,D′,P; Fig. S3, Table S1). As we used an antibody that recognizes total β-catenin, a complex pattern was observed at s7, with membrane-associated and cytoplasmic pools, and some immunopositive nuclei that begin to be distinguished (Fig. S3). We obtained mixed results for total β-catenin IF quantification at this stage (Fig. 1, Fig. S3, Table S1). However, in some s7 embryos, it appeared that the enrichment of Notch1 IF in the apical region of the ventral-most animal cells was complemented with lower levels of β-catenin IF, compared with the basal region of these cells, or with dorsal cells exhibiting a more uniform distribution of β-catenin (see cryosections in Fig. 1D,H,L and Fig. S3E-N). In other embryos, we noticed the weakest β-catenin IF in the nuclear region of the ventral-most cells with the highest levels of Notch1 IF (whole-mount hemisection, Fig. S3A-D″). In addition, it is known that dorsal accumulation of transcriptionally active nuclear β-catenin is best detected at s8 (Schohl and Fagotto, 2002). The higher cell number and smaller cell size helped to obtain more DAPI$^+$ nuclei in the same plane at this stage. Analysis of images with a high enough resolution to quantify IF intensity at the cellular level (see cryosection in Fig. 1M-O,Q-U) and analysis of the IF patterns in whole-mount hemisections (Fig. S4) showed a consistent opposite distribution of both proteins at s8, with dorsal enrichment of total and nuclear β-catenin and ventral enrichment of total and nuclear Notch1 (Tables S1 and S2).

To verify the distribution of Notch1 protein in the DV axis, we performed a combined assay of Notch1 IF with ISH of known dorsal markers, such as *wnt11* for early cleavage (Tao et al., 2005) and *chordin* for s8 (Kuroda et al., 2004). We found that, in 96% of the cases (n=23), they were clearly expressed at the opposite side in relation to Notch1 (Fig. 2B-G″, Table S3A,B). This higher frequency of ventral Notch1 location, in comparison with that found in the experiments in which we employed the pigmentation criterion described in the Materials and Methods section (Klein, 1987), is because the orientation of the embryos was more accurately assigned by the dorsal marker than by the pigmentation pattern. These results confirm that Notch1 protein is enriched in the ventral side from s1 to mid-blastula.

We conclude that Notch1 protein is consistently enriched in the ventral region from the beginning of embryogenesis in *Xenopus*. Opposite patterns of Notch1 and β-catenin in the DV axis are consistently evident around the mid-blastula transition, when the strongest nuclear β-catenin accumulation is found on the dorsal side of the embryo, as previously reported (Schohl and Fagotto, 2002).

In addition, we performed double IF with the same antibodies in the more transparent zebrafish embryos, which initially develop as a disc over a large yolk cell. We found an asymmetric distribution of Notch1 protein from the one-cell stage until the blastula (which was the last stage analyzed) in 88% of the embryos (Fig. 3, Table S4), which showed an opposite distribution to β-catenin IF. Although the polarity of the initial DV axis cannot be predicted from the cleavage pattern in zebrafish, accumulation of nuclear β-catenin marks the dorsal side in blastulae (Schneider et al., 1996). At this stage, total β-catenin and nuclear β-catenin were enriched in the region opposite to that in which the strongest Notch1 IF was observed (Fig. 3L-O). This indicates that the Notch1 ventral enrichment is conserved during early embryogenesis in both *Xenopus* and zebrafish embryos.

Notch1 mRNA is ventrally located from the beginning of *Xenopus* embryogenesis

To begin to understand why Notch1 protein is asymmetrically distributed from the beginning of embryogenesis, we first analyzed the distribution of *notch1* mRNA in pigmented left halves of *Xenopus* embryos. Notably, we found that *notch1* mRNA was enriched in the ventral region in relation to the dorsal side from s1 to the last stage analyzed (s8) in 87% of embryos from three independent batches (Fig. 2H-M; Table S5). We also performed RT-qPCR analysis of *notch1* and *wnt11* mRNA on samples extracted from dorsal and ventral halves from another two independent batches of embryos (Fig. 2N). In both, *wnt11* was significantly enriched in the dorsal half at s5, as has previously been described (Fig. 2N, right) (Tao et al., 2005). In contrast, *notch1* mRNA levels were significantly higher in the ventral half samples than in the dorsal

Development (2018) 145, dev159368. doi:10.1242/dev.159368

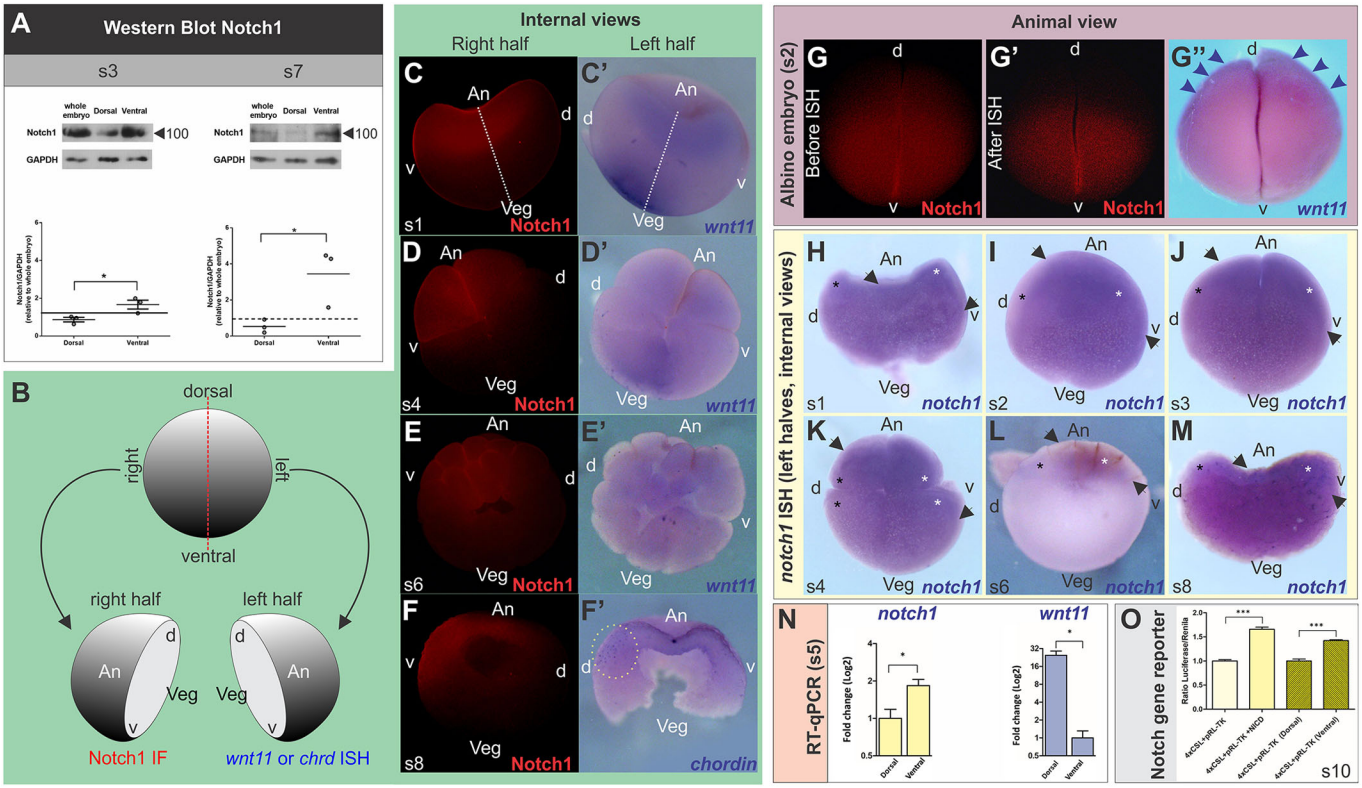

Fig. 2. The levels of Notch1 protein and mRNA and of CSL-dependent transcriptional activity are higher in the ventral side of *Xenopus* embryos. (A) Western blot of Notch1 in protein extracts from whole embryos and from dorsal and ventral halves at s3 and s7. At these stages, the more representative p100 band was quantified relative to GAPDH levels. Significantly higher levels of Notch1 protein were detected in ventral halves than in dorsal halves at both stages. **P*<0.05 (*t*-test, from three independent experiments). Horizontal lines represent the mean values between the experiments; circles show the results for each experiment. (B-F′) Left and right halves of pigmented embryos were cut (B, dashed red line) at the indicated stages and processed as indicated for whole-mount IF of Notch1 (right halves; C-F), or for ISH of dorsal markers in contralateral left halves (*wnt11* in C′-E′, *chordin* in F′). Notch1 IF is highest on the opposite side to the dorsal markers. The dotted white line in C,C′ shows the animal-vegetal axis. The dotted yellow circle in F′ shows the population of dorsal cells that are beginning to express *chordin* at this stage. (G-G″) The same albino two-cell embryo was processed for Notch1 IF and *wnt11* ISH. Notch1 IF is shown in animal view before (G) and after (G′) ISH, and it is higher on the opposite side in relation to the early dorsal marker *wnt11* (G″, arrows). (H-M) Left halves of embryos were cut at the indicated stages and processed for ISH of *notch1*. A higher expression of *notch1* transcripts was observed in the ventral (white asterisks) than in the dorsal region (black asterisks). The arrows indicate the approximate dorsal and ventral limits of the *notch1* domain. (N) RT-qPCR quantification of *notch1* and *wnt11* mRNA in dorsal and ventral halves of s5 embryos. *Notch1* mRNA levels were significantly higher in the ventral halves, and *wnt11* mRNA levels were significantly higher in the dorsal halves (**P*<0.05, one-way ANOVA). (O) Notch reporter gene analysis of CSL-dependent activity. Relative luciferase/*Renilla* activity was significantly increased by *nicd1* mRNA (NICD) and was significantly higher in the ventral half than in the dorsal half of s10 embryos. Data are mean +s.e.m. ****P*<0.05 [one-way ANOVA analysis and Bonferroni's multiple comparisons test (Student's *t*-test)]. s, stage.

ones (Fig. 2N, left), confirming that it is enriched in the ventral region during early cleavage.

Notch/CSL-dependent activity is higher in the ventral side

The previous results show that both Notch1 mRNA and protein are enriched ventrally. In addition, we were able to detect Notch1^{+} nuclei in the ventral side at cleavage/mid-blastula stages, suggesting that Notch1 protein might be ready to activate transcription. To see whether there is endogenous asymmetric Notch/CSL-dependent activity across the DV axis, we performed a CSL-luciferase reporter assay at the onset of gastrulation. Constitutively active *nicd1* mRNA increased the reporter activity in three independent experiments, with significant differences between *nicd1* and controls in two of the three experiments (Fig. 2O, left pair of bars), indicating that the assay is sensitive to measuring Notch/CSL-dependent activity in *Xenopus* embryos. The assay also detected higher endogenous CSL-reporter activity in the ventral halves compared with the dorsal halves in the three independent experiments, with significant differences in two of them (Fig. 2O, right pair of bars). These results indicate that CSL-dependent transcription is higher in the ventral side at the beginning of gastrulation.

Notch1 is necessary for the expression of genes of the ventral program

Next, we investigated whether *notch1* could control the expression of VC genes. We performed gain- and loss-of-function experiments and analyzed the expression of *Xenopus* ventral markers by ISH around the onset of gastrulation (*wnt8a*, *vent-2b*) or at mid/late gastrula for *bmp4*, as this marker is not well detected by this method at earlier stages. Injection of *nicd1* mRNA, which encodes the constitutively transcriptionally active intracellular domain of Notch1 (Chitnis et al., 1995), increased or expanded the expression domains of *wnt8a* (81%; Fig. 4A-D,K) and *vent-2b* (87%; Fig. 5A-D,K). *Bmp4* was upregulated in some cases (44%; Fig. 6A,B, green asterisk; Fig. 6M) it was downregulated in others (48%; Fig. 6A,D, red asterisk; Fig. 6M) and it was unaffected in a small proportion of injected embryos (8%; Fig. 6A,C, yellow asterisk). Overexpression of the full-length *notch1* mRNA (*notch1 FL*) upregulated the three

Development (2018) 145, dev159368. doi:10.1242/dev.159368

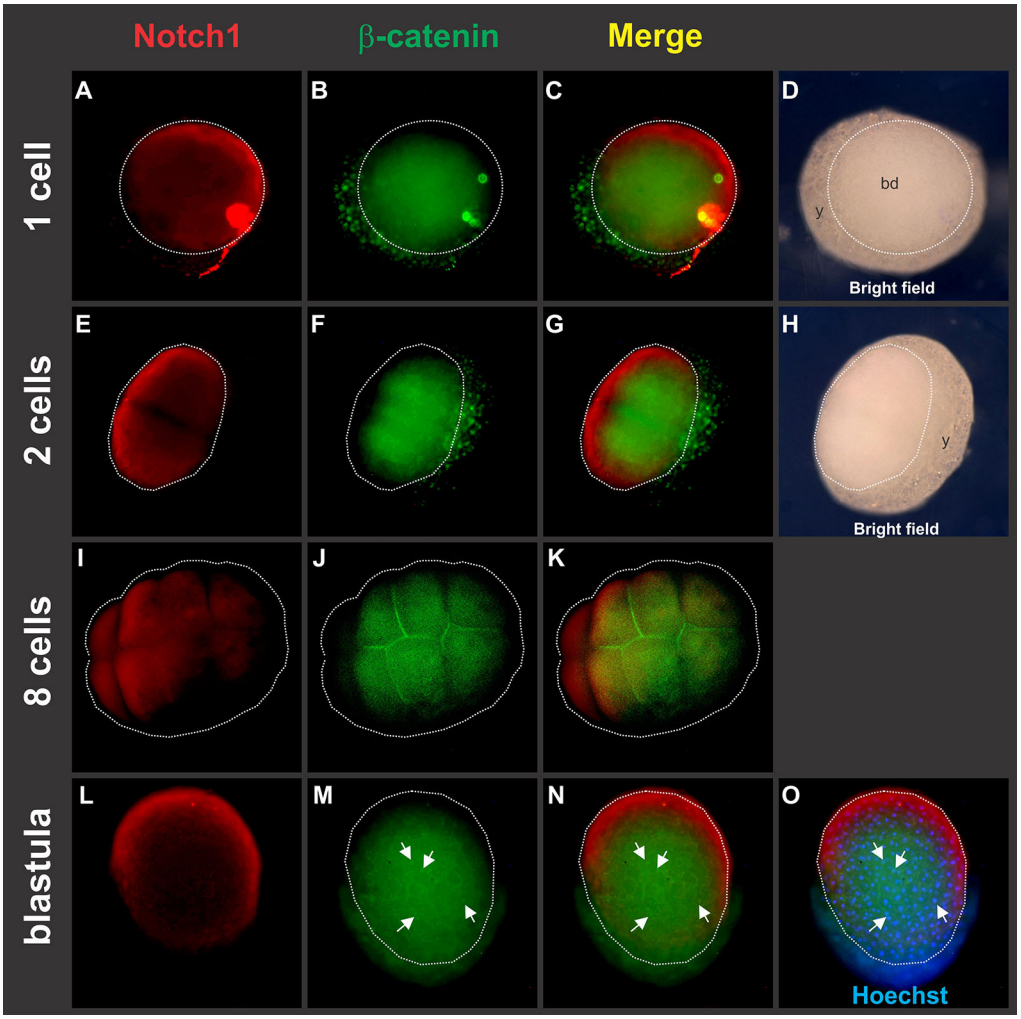

Fig. 3. Distribution of endogenous Notch 1 and β-catenin proteins in zebrafish embryos. (A-O) Animal views of zebrafish embryos at the indicated stages (Kimmel et al., 1995) showing Notch1 IF (A,E,I,L), total β-catenin IF (B,F,J,M) and merged images of Notch1 and total β-catenin IF (C,G,K,N). D and H show bright-field views of the one-cell and two-cell stages, respectively, indicating the blastodisc (bd, demarcated by the dotted white line) and yolk cell (y). (O) Merged image of nuclear Hoechst (blue) with Notch1 and total β-catenin IF. White arrows point to nuclear β-catenin in M-O.

ventral markers (91% for *wnt8a*, Fig. 4E,F,K; 91% for *vent-2b*, Fig. 5E,F,K; 82% for *bmp4*, Fig. 6E,F,M). In contrast, Notch1 Mo consistently decreased their expression (93% for *wnt8a*, Fig. 4G,H,K; 88% for *vent-2b*, Fig. 5G,H,K; 100% for *bmp4*, Fig. 6G,H,M). In addition, we injected *su(H)1*^{DBM} mRNA to impair CSL-dependent, canonical Notch activity (Wettstein et al., 1997). This resulted in a consistent downregulation of *wnt8a* (93%, Fig. 4I-K) and *vent-2b* (77%, Fig. 5I-K), but the effect on *bmp4* expression was more variable (27% unaffected, 50% downregulated, 23% upregulated on the injected side; Fig. 6I-M).

Three additional independent experiments were carried out using RT-qPCR, to verify the effect of Notch manipulation on ventral markers. Data are shown in Fig. 4L, 5L, 6N and Fig. S6F-J. Consistent with the ISH results for *wnt8a and vent-2b*, both Notch1 Mo and *su(H)1*^{DBM} significantly downregulated all the ventral markers analyzed at early gastrula stage (Fig. 4L and 5L), including *bmp4* (Fig. 6N), which was not analyzed by ISH at this stage because it is not well detected by this method at early gastrula. Notch1 Mo kept these markers downregulated at mid gastrula, whereas *nicd1* mRNA was able to upregulate them (Fig. 4L and Fig. S6F for *wnt8a*; Fig. 5L for *vent-2b* and *ventx2.2*; Fig. 6N for *bmp4*).

For one of the RT-qPCR experiments, we also co-injected Notch1 Mo with *nicd1* mRNA and assessed the effect on *wnt8a* at s11, when the Notch target gene *hes9.1* (which we used as a control of Notch responsiveness) is well expressed. *Nicd1* mRNA rescued the downregulation of *wnt8a* and *hes9.1* produced by Notch1 Mo (Fig. S6F and G, respectively), indicating that the effects of Notch1 Mo were specific. This rescue was confirmed by *wnt8a* ISH in another two independent experiments (Fig. S6A-E). In addition, Notch1 Mo downregulated other genes important for the ventral program, such as *trim29* (Hayes et al., 2007; Cibois et al., 2015; Popov et al., 2017) (Fig. S6H), *xk81a1* (Yan et al., 2009; Scerbo et al., 2017) (Fig. S6I) and *tfap2a* (Luo et al., 2002) (Fig. S6J). *Nicd1* mRNA also rescued the effect of Notch1 Mo on these genes (Fig. S6H-J), further confirming the specificity of Notch1 Mo, and that the ventral program requires an intact *notch1* function. In conclusion, our results indicate that Notch1 is required for the normal expression of genes with essential roles in the ventral program.

DISCUSSION

In the present work, we show for the first time that Notch1 protein is enriched in the ventral region from the beginning of embryogenesis in both *Xenopus* and zebrafish (Fig. 7). Our results suggest that a mechanism that controls *notch1* mRNA localization underlies this asymmetry of Notch1 protein.

Notch1 establishes an opposite distribution in relation to dorsal nuclear β-catenin at blastula stages, consistent with our previous hypothesis of a Notch1-mediated destabilization of transcriptionally active β-catenin in the ventral side (Fig. 7, route 1). Further work is needed to understand how this mechanism operates at the cellular level. β-Catenin is involved in complex intracellular dynamics, is distributed in different pools, and is regulated by phosphorylation

Development (2018) 145, dev159368. doi:10.1242/dev.159368

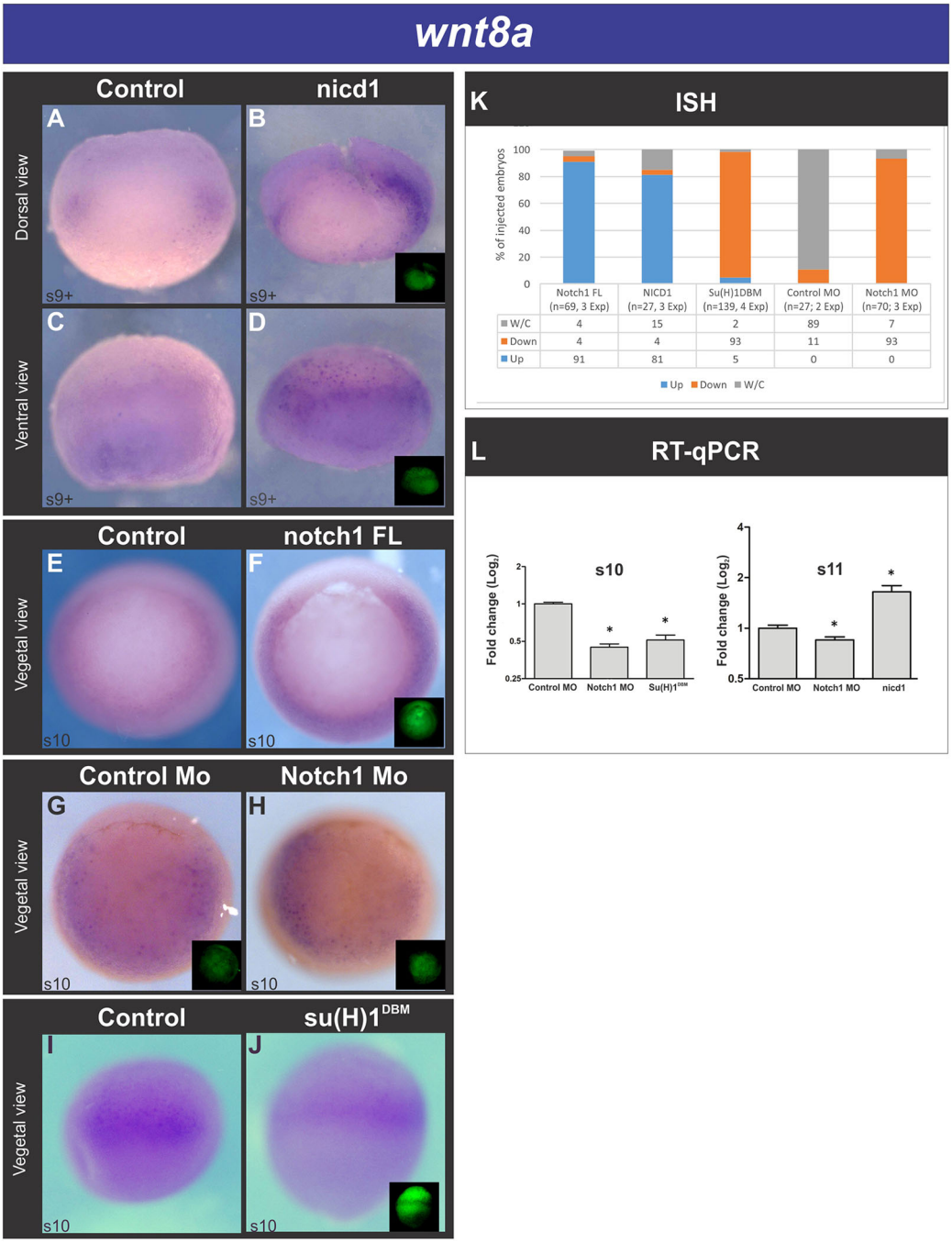

Fig. 4. *Notch1* is necessary for the expression of the ventral center gene *wnt8a*. (A-J) ISH expression pattern of *wnt8a* mRNA in embryos in which the Notch pathway was stimulated (B,D,F), or blocked (H,J), and in their corresponding sibling uninjected controls (A,C,E,I) or control Mo-injected sibling (G). Insets show the green fluorescence of the co-injected tracer DOG. (B,D) Embryos injected with 1 ng of *nicd1* mRNA when the first cleavage was incipient. Note the upregulation and the dorsalwards expansion of *wnt8a* expression on the injected side in the dorsal view (B), whereas in the ventral view (D), where the tracer is more evenly distributed between the left and the right side of the embryo, *wnt8a* is strongly upregulated in comparison with the uninjected sibling control (C). (F) Embryo injected with 1 ng of *notch1 FL* mRNA at the one-cell stage. The expression of *wnt8a* was consistently stronger than in uninjected sibling controls (E). (G,H) Sibling embryos unilaterally injected with 40 ng of control Mo (G) or with 40 ng of Notch1 Mo (H) when the first cleavage was incipient. Note the downregulation of *wnt8a* towards the injected side in H. *Wnt8a* expression in control Mo-injected siblings was essentially unaffected. (J) Embryo injected with 2 ng of *su(H)1*^{DBM} mRNA at the one-cell stage. The expression of *wnt8a* was consistently weaker than in uninjected sibling controls (I). (K) Summary of ISH results, expressed as the percentage of embryos showing the changes in *wnt8a* expression, indicated by the color codes [cyan, upregulated; orange, downregulated; gray, without changes (W/C)]. The number of total embryos analyzed (*n*) and the number of independent experiments (Exp) are indicated for each bar. (L) Quantification of *wnt8a* mRNA by RT-qPCR at s10 and at s11. Data are mean+s.e.m. *P<0.05 (one-way ANOVA analysis compared with control Mo injection). s, stage.

and interactions with cadherins, which all complicate the analysis (McCrea et al., 2015; Muñoz-Descalzo et al., 2015). We found that, whereas Notch1 is consistently enriched in the ventral region from the beginning of embryogenesis in all stages analyzed, the global distribution of total β-catenin was more variable in *Xenopus* until s7. However, in some s7 embryos we noticed an opposing distribution of

Development (2018) 145, dev159368. doi:10.1242/dev.159368

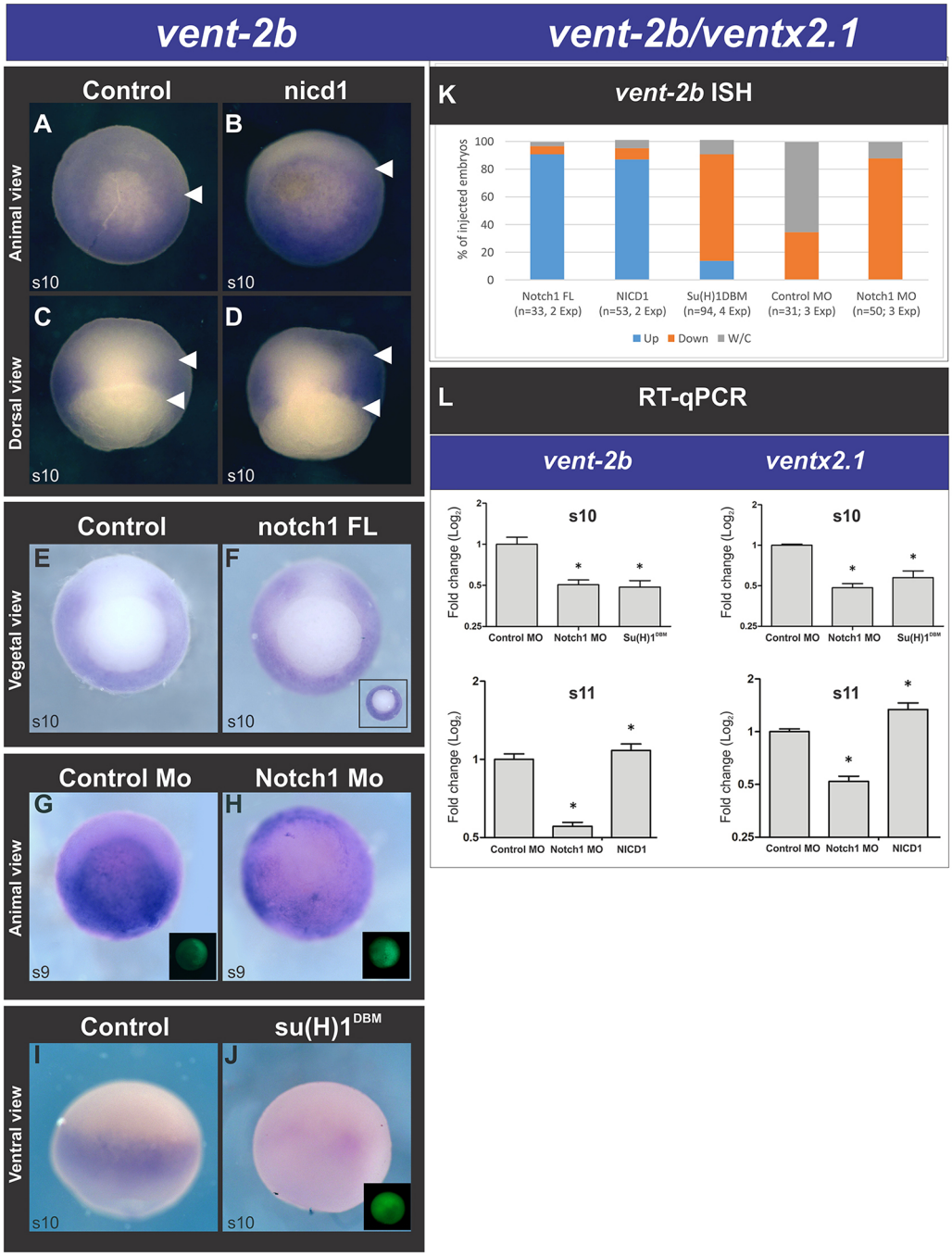

Fig. 5. *Notch1* is necessary for the expression of ventral center genes of the Ventx family. (A-J) ISH expression pattern of *vent-2b* mRNA in embryos in which the Notch pathway was stimulated (B,D,F) or blocked (H,J), and in their corresponding sibling uninjected controls (A,C,E,I) or control Mo-injected sibling (G). Insets show the green fluorescence of the co-injected tracer DOG. (B,D) Embryos injected with 1 ng of *nicd1* mRNA when the first cleavage was incipient. Note the expansion of *vent-2b* expression in comparison with the uninjected sibling controls (A,C), indicated by arrowheads. (F) Embryo injected with 1 ng of *notch1 FL* mRNA at the one-cell stage. The expression of *vent-2b* was expanded towards the dorsal side in most embryos (95%, *n*=19) in comparison with uninjected sibling controls (E), occasionally occupying completely the dorsal region, as shown in inset (10% of the injected embryos). (G,H) Sibling embryos unilaterally injected with 30 ng of control Mo (G) or with 30 ng of Notch1 Mo (H) when the first cleavage was incipient. Note the downregulation of *vent-2b* towards the injected side. (J) Embryo injected with 4 ng of *su(H)1*^{DBM} mRNA at the one-cell stage. The expression of *vent-2b* was consistently weaker than in uninjected sibling controls (I). (K) Summary of ISH results, expressed as the percentage of embryos for the changes in *vent-2b* expression, indicated by the color codes [cyan, upregulated; orange, downregulated; gray, without changes (W/C)]. The number of total embryos analyzed (*n*) and the number of independent experiments (Exp) are indicated for each bar. (L) Quantification of *vent-2b* (left) and *ventx2.1* (right) mRNAs by RT-qPCR at s10 and s11. Data are mean+s.e.m. **P*<0.05 (one-way ANOVA analysis compared with control Mo injection). s, stage.

Notch1 and β-catenin proteins in ventral-animal cells. Notch1 was enriched in the apical region, but β-catenin levels increased towards the basal region. Interestingly, it has been proposed that, in the absence of Wnt signaling, Notch sequesters a cell surface-located pool of transcriptionally active Armadillo/β-catenin and induces its degradation in *Drosophila*. In this way, Notch functions as a buffer against fluctuations in the levels of transcriptionally active Armadillo/β-catenin that leaks from the Gsk-3β-dependent

Development (2018) 145, dev159368. doi:10.1242/dev.159368

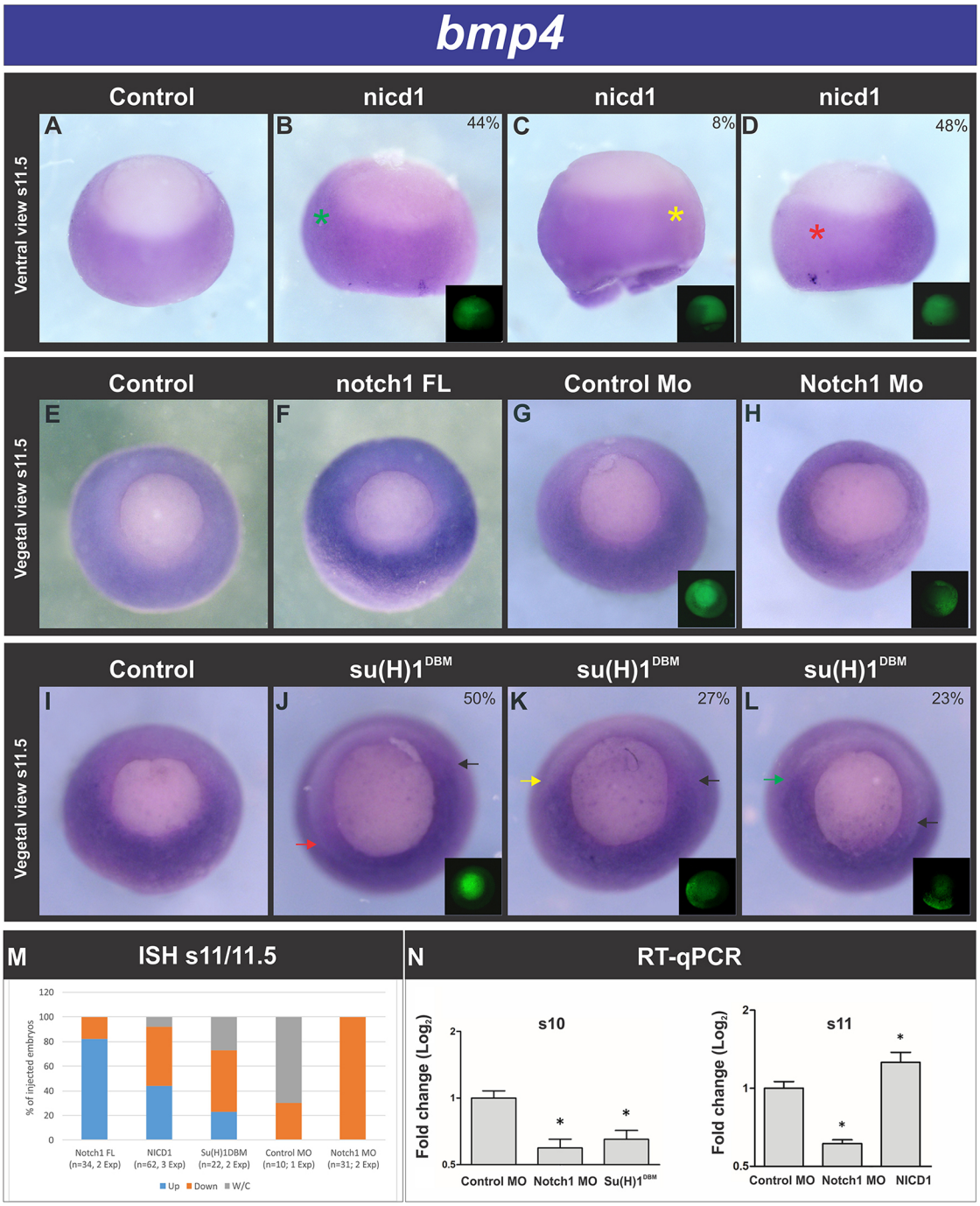

Fig. 6. Effects of manipulating Notch1 activity on the ventral center gene *bmp4*. (A-L) ISH expression pattern of *bmp4* in embryos in which the Notch pathway was stimulated (B-D,F) or blocked (H,J-L). Corresponding sibling uninjected controls (A,E,I) or control Mo-injected sibling (G). Insets show the green fluorescence of the co-injected tracer DOG. (B-D) Embryos unilaterally injected with 1 ng of *nicd1* mRNA into one cell at the two-cell stage. *Bmp4* was upregulated on the injected side in comparison with the non-injected side in some cases (B, 44%, *n*=62; green asterisk), but it was downregulated in others (D, 48%, *n*=62; red asterisk) and it was unaffected in a low proportion of the injected embryos (C, 8%, *n*=62; yellow asterisk). (F) Embryo injected with 1 ng of *notch1 FL* mRNA at the one-cell stage, showing the strong upregulation of *bmp4* in comparison with uninjected sibling controls (E). (G,H) Sibling embryos unilaterally injected with 30 ng of control Mo (G) or with 30 ng of Notch1 Mo (H) into one cell at the two-cell stage. *Bmp4* was completely downregulated on the injected side in H. (J-L) Unilateral injection of 1 ng of *su(H)1*^{DBM} mRNA into one cell at the two-cell stage leads to variable results in *bmp4* expression when comparing the injected- with the non-injected side: (J) 50% downregulated (red arrow), (K) 27% unaffected (yellow arrow), (L) 23% upregulated (green arrow). Black arrows point to the dorsal/ventral limit of the *bmp4* domain on the non-injected side. (M) Summary of ISH results, expressed as the percentage of embryos showing the changes in *bmp4* expression indicated by the color codes [cyan, upregulated; orange, downregulated; gray, without changes (W/C)]. The number of total embryos analyzed (*n*) and the number of independent experiments (Exp) are indicated for each bar. (N) Quantification of *bmp4* mRNA by RT-qPCR at s10 and s11. Data are mean+s.e.m. **P*<0.05 (one-way ANOVA analysis compared with control Mo injection). s, stage.

destruction complex (Sanders et al., 2009). The variability that we found in the DV distribution of total β-catenin at early stages might be indicative of such fluctuations during the process of Notch buffering.

We also found that Notch1 is required for the normal expression of genes essential for a fully functional ventral program. Notch1 is able to positively control ventral genes in a CSL-dependent fashion

Development (2018) 145, dev159368. doi:10.1242/dev.159368

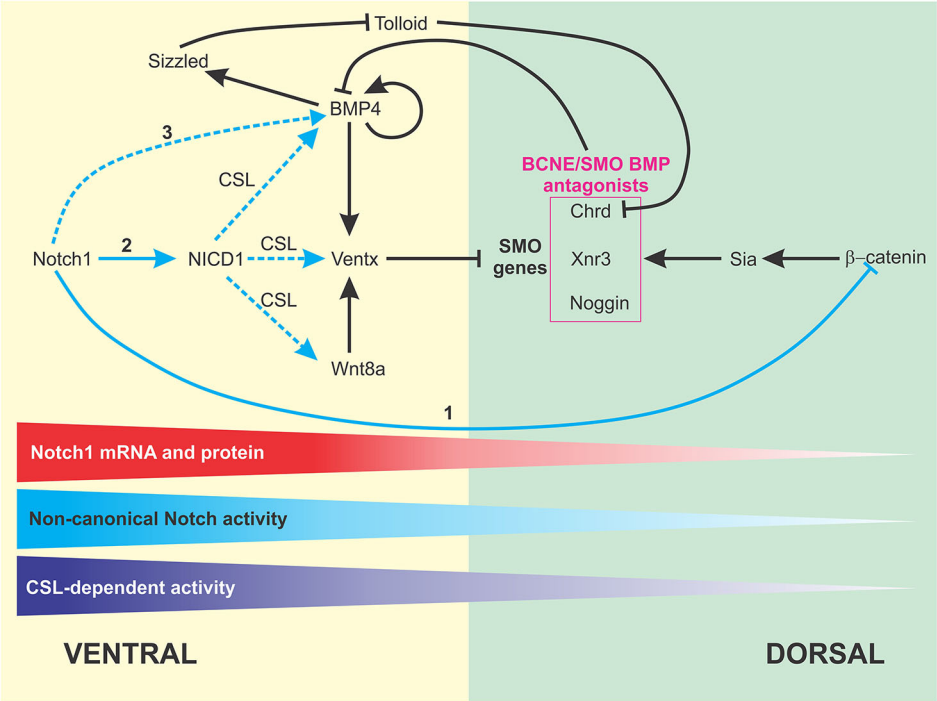

Fig. 7. Proposed model for the role of Notch1 in ventral development. Notch protein and mRNA are present in higher levels ventrally than dorsally (this work; red triangle). Ventrally enriched Notch1 participates in the control of the initial DV polarity by a dual mechanism (turquoise lines): by destabilizing the dorsal determinant β-catenin (Acosta et al., 2011; non-canonical Notch activity, turquoise triangle; route 1); or by promoting the development of the VC (this work; route 2). CSL-dependent transcriptional activity is higher ventrally than dorsally at the onset of gastrulation (this work; blue triangle). Notch1 is necessary for the expression of the ventral morphogens Wnt8a and BMP4, and the Ventx family transcriptional repressors, which are regulated in a CSL-dependent fashion around the onset of gastrulation (route 2). The dashed turquoise arrows indicate positive regulation by Notch1 on VC genes, but it remains to be answered whether it is direct or indirect. Notch1 might positively control *bmp4* indirectly, by contributing to the destabilization of β-catenin in the ventral side (route 2), thus preventing the expression of BMP antagonists in this region, which otherwise would interrupt the known positive feedback loop by which *bmp4* increases its own expression; however, we cannot rule out that Notch1 regulates *bmp4* by other pathways (route 3). BCNE, blastula *chordin* and *noggin* expressing center; SMO, Spemann–Mangold's organizer. See main text for further explanation.

around the onset of gastrulation (Fig. 7, route 2), although we do not know whether it does it in a direct or indirect way (Fig. 7, dashed lines). Intriguingly, ISH analysis at mid/late gastrula revealed that constitutively active *nicd1* and blockade of canonical CSL-dependent activity produced variable results for *bmp4*. This might be related to time-dependent changes, as it is known that Notch signaling can elicit opposite effects depending on time and context (Glavic et al., 2004; Contakos et al., 2005; Revinski et al., 2010). Notch1 might also positively control *bmp4* indirectly, by contributing to the destabilization of β-catenin in the ventral side (Fig. 7, route 1), thus preventing the expression of BMP antagonists in this region, which would otherwise interrupt the known positive feedback loop by which *bmp4* increases its own expression (De Robertis, 2009) (Fig. 7). The situation could be more complex because *bmp4* is deeply involved in an intricate network of biochemical interactions between the dorsal and ventral centers that self-regulates the DV field. *bmp4* is able to indirectly decrease its own expression by upregulating *sizzled*, an inhibitor of the Tolloid metalloproteinase that degrades Chordin. If BMP levels increase, *sizzled* expression is enhanced, thus leading to an increase in Chordin levels, which results in inhibition of BMP signaling by blocking BMP function, decreasing its levels by interrupting the BMP positive-feedback loop (De Robertis, 2009) (Fig. 7). Thus, it is conceivable that, in our experimental conditions, if *nicd1* tends to upregulate *bmp4*, and BMP4 reaches a threshold, the self-regulatory network might operate, attempting to downregulate *bmp4*. This might, in part, underlie the mixed results that we obtained by ISH for *bmp4* expression at mid/late gastrula. Notch-dependent β-catenin degradation has been shown to be primarily elicited by membrane-tethered uncleaved Notch in other systems (Hayward et al., 2005; Kwon et al., 2009). If *notch1 FL* is stronger than *nicd1* in promoting β-catenin degradation, this effect would prevent the operation of the self-regulatory network that balances *bmp4* expression, as it depends on β-catenin signaling. If this is the case, the upregulation of *bmp4* by *notch1 FL* would prevail. This might explain the differences in the response of *bmp4* to *nicd1* and *notch1 FL*. These kinds of mechanisms are difficult to show using RT-qPCR, as it measures the mean levels of mRNA in a population, thus masking the variabilities of response that occur within the population, which can be analyzed by ISH in individual phenotypes.

The downregulation of ventral markers by *su(H)1*^{DBM} mRNA around the onset of gastrulation, and the higher CSL-dependent transcriptional activity in the ventral side at early gastrula, revealed by the gene reporter assay that we show here, support the hypothesis of a spatial regulation of canonical Notch activity in the DV axis. In addition, we have previously shown that *notch1* restricts the expression of *chordin* and *Xnr3* in the BCNE in a CSL-independent fashion by promoting β-catenin degradation (Acosta et al., 2011). We propose that Notch1 canonical and non-canonical activity is spatially regulated in the animal hemisphere, with lower levels at the dorsal side and higher levels at the ventral side. An unknown mechanism controlling Notch1 mRNA and protein distribution from the beginning of embryogenesis underlies this process (Fig. 7).

Development (2018) 145, dev159368. doi:10.1242/dev.159368

It will be important to elucidate how Notch1 controls the expression of ventral genes. Although the most studied Notch targets are the HES/HEY genes, which encode transcriptional repressors of the bHLH family, other targets are beginning to emerge in different animal models, including genes involved in proliferation (such as *Myc*, *Cyclin D*), apoptosis (*reaper*, *hid*), cell fates (*Gata3*, *Pax2*), signaling pathways (*lip-1*, *ERBB2*, *EGFR*, *Notch*), metabolism and cytoskeletal regulators (Bray and Bernard, 2010). Strikingly, GATA factors are required for *wnt8a* and *ventx1.2* but not for *bmp4* and *ventx2.2* expression in *Xenopus* (Sykes et al., 1998). Interestingly, a link between *notch* and *wnt8* has recently been revealed in posterior development in short-germ arthropods, in which posterior segments are added sequentially from a segment addition zone that requires a positive regulation of *wnt8* by Delta-Notch signaling to develop (Schönauer et al., 2016). Comparative studies indicated that the common ancestor of arthropods employed *delta-notch*, *wnt8* and *caudal* for posterior development and it was suggested that this gene regulatory network was already present in the common ancestor of arthropods and vertebrates (Urbilateria) (McGregor et al., 2009).

Final conclusions

Although it is well accepted that relocation of dorsal determinants soon after fertilization activates the maternal Wnt/β-catenin pathway that drives the development of the dorsal center, it remained unclear whether an analogous event of asymmetric distribution of ventral determinants occurs in the earliest stages of development. Overall, there is no published evidence of early asymmetries of maternal components of the BMP signaling pathway before the mid-blastula transition. While zygotic components of the ventral cascade start to be transcribed at the mid-blastula stage, they are initially expressed in a uniform fashion and become restricted to the VC during gastrulation (Ventx genes), or they begin to be expressed ventrally at blastula stages (*wnt8a*) or at the mid-gastrula stage (*bmp4*) (see Introduction). To our knowledge, ventral enrichment of Notch1 mRNA and protein is the earliest localized sign of ventral development reported in vertebrates, preceding the appearance of the strong localized expression of *wnt8a*, *bmp4* and Ventx genes in the VC, and the dorsal accumulation of transcriptionally active nuclear β-catenin in the opposite region. Together with our previous findings (Acosta et al., 2011), our results indicate that during early embryogenesis, ventrally located Notch1 participates in the control of the initial DV polarity by a dual mechanism: (1) by promoting the development of the VC and (2) by destabilizing transcriptionally active β-catenin (Fig. 7).

MATERIALS AND METHODS

Embryological manipulations, RNA synthesis, morpholinos and injections

Albino and wild-type *Xla* embryos were obtained using standard methods (Franco et al., 1999) from adult animals obtained from Nasco, and staged according to Nieuwkoop and Faber (1994). *Danio rerio* (zebrafish) embryos were obtained as previously described (Kamm et al., 2013) and staged according to Kimmel et al. (1995). *Xenopus laevis* in S.L.L.'s laboratory and *Danio rerio* in L.F.F.'s laboratory were employed according to protocols approved by the Laboratory Animal Welfare and Research Committees (CICUAL) from Facultad de Medicina-UBA and INGEBI-CONICET, respectively. Experiments on *Xenopus laevis* in L.K.'s laboratory were approved by the 'Direction départementale de la Protection des Populations, Pôle Alimentation, Santé Animale, Environnement, des Bouches du Rhône' (agreement number F 13 055 21). All experiments were performed following Directive 2010/63/EU of the European Parliament and of the council of 22 September 2010 on the protection of animals used for scientific purposes.

Synthetic capped mRNAs for microinjections were obtained as follows. *Xla notch1* full length in pSP72 (*notch1 FL*) (Coffman et al., 1990) was digested with *Xho*I and *in vitro* transcribed with the T7 Megascript transcription kit (Ambion, AM1334) with a 4:1 cap analog:GTP ratio, using m7G(5′)ppp(5′)G (Ambion, AM8050). *Xla nicd1* pCS2+MT and *Xla su(H)1*^{DBM} pCS2+MT (Chitnis et al., 1995; Wettstein et al., 1997) were digested with *Not*I and *in vitro* transcribed with the mMESSAGE mMACHINE SP6 Transcription Kit (Ambion, AM1340). Capped mRNAs were purified with the RNeasy mini kit (Qiagen, 74104).

The *notch1* antisense morpholino oligonucleotide (Notch1 Mo) with the base composition 5′-GCACAGCCAGCCCTATCCGATCCAT-3′ has previously been used and validated in works by our group and by other authors (López et al., 2003; Revinski et al., 2010; Acosta et al., 2011; Sakano et al., 2010). As control morpholino (control Mo), we used the standard control oligo or the random control oligo 25-N (Gene Tools). Each embryo was injected with 30-40 ng of the relevant Mo.

Embryos were injected in the animal hemisphere at the one-cell stage, or unilaterally, from early to late two-cell stage, as detailed in the figures. Injections included as tracer 20-40 ng of Dextran Oregon Green 488, MW 10000, anionic lysine fixable (DOG; Thermo Fisher Scientific, D7171).

For gain- and loss-of-function studies in *Xenopus*, sibling embryos were randomly allocated to control or experimental groups. Results are expressed as percentage of the total number (*n*) of embryos with the indicated phenotypes, which are described in the main text, in the figure legends or in the supplementary tables.

In situ hybridization and immunolocalization

The preparation of digoxigenin-labeled antisense RNA probes and the whole-mount ISH were performed as previously described (Pizard et al., 2004), except that the proteinase K step was omitted. Probes for *wnt8a*, *vent-2b*, *bmp4*, *wnt11* and *chordin* have been described previously by other authors (Christian and Moon, 1993; Rastegar et al., 1999; Fainsod et al., 1994; Freeman et al., 2008; Saka et al., 2000; Kuroda et al., 2004).

For immunodetection of endogenous Notch1 and β-catenin proteins or of NICD1 protein after injection of *nicd1* mRNA, *Xenopus* embryos were fixed for 90 min with MEMPFA and then transferred to Dent's fixative (80% methanol, 20% DMSO) for 72 h at 4°C or −20°C. To orient the embryos in the DV axis, we cut left and right halves of regularly cleaving embryos from batches in which the paler pigmentation zone was bisected by the first cleavage furrow, as the paler region predicts the prospective dorsal side with ∼70% accuracy in *Xla* (Klein, 1987). Left and right halves, or animal halves, when required, were cut after rehydration. Afterwards, embryos were further processed as previously described, including a bleaching step to avoid quenching of the IF signal by the pigment (Acosta et al., 2011).

For preparing samples for cryosections, left and right embryo halves treated as previously described were impregnated in 15% sucrose in 1× PBS for 30 min at room temperature, and were then kept overnight in 30% sucrose in 1× PBS at 4°C. The following day, specimens were incubated in 15% gelatin (Sigma, G9391) in 1× PBS for 30 min at 37°C, in 2 ml tubes. Embedding was performed in the same solution, and specimens were oriented in such way that the internal surface of the embryo halves were laid on the bottom. In this way, serial sections were obtained, with the first section being the most internal. Embedded specimens were snap-frozen by immersion for 1 min in an isopropanol/dry ice bath at −40°C or below, and immediately transferred to −70°C overnight. Before sectioning, specimens were transferred to −20°C for 1 h. Sections of 20 µm thickness were obtained with a cryostat (Leica, CM1850) and collected on positively charged glass slides (Fisherbrand, Superfrost Plus). Sections were dried overnight at room temperature.

Immunodetection was performed in general as previously described for whole-mount specimens (Acosta et al., 2011), except that for sections, incubations were carried out with 0.2 ml of each solution per slide, the slides being covered with Parafilm. Antibody incubations were performed overnight at 4°C in a wet chamber, and the antibodies were washed four times for 30 min with 50 ml 1× PBS each. Slides were mounted with Vectashield containing DAPI (Vector Laboratories, H-1200).

Zebrafish embryos were fixed and processed for whole-mount IF in the same conditions as *Xenopus* embryos, except that, after rehydration,

Development (2018) 145, dev159368. doi:10.1242/dev.159368

they were dechorionated with sharp forceps before proceeding to IF of whole embryos.

The commercially available Notch1 intra rabbit polyclonal antibody (N1 intra Ab) (Abcam, ab8387) was raised against a peptide from the human intracellular domain of NOTCH1, which has 93% identity with the protein encoded by *Xla notch1*. In human breast tumors, the antibody detects both nuclear and cytoplasmic NOTCH1 in tissue sections (Efstratiadis et al., 2007).

Primary and secondary antibodies were diluted in blocking buffer as follows: β-catenin (mouse monoclonal IgG, which recognizes total β-catenin; Abcam, ab19448, 1/100), N1 intra Ab (1/200), anti-rabbit IgG-HRP (Santa Cruz Biotechnology, sc-2004, 1/1000), anti-rabbit IgG-Alexa 594 (Thermo Fisher Scientific, A-11012, 1/100), anti-mouse IgG F(ab′)2-Alexa Fluor 488 (Thermo Fisher Scientific, A-11017, 1/200). For double IF for Notch1 and β-catenin in whole-mount hemisections, we restricted the comparison of both patterns to those embryos in which Notch1 was enriched in the ventral region, according to the orientation predicted by pigmentation.

Whole embryos and cryosections were photographed in a MVX10 fluorescence microscope (Olympus) equipped with a DP72 camera (Olympus). Higher resolution IF and DAPI images for quantitative analysis at s8 were photographed in an inverted motorized fluorescence microscope IX83 (Olympus) equipped with a Hamamatsu C11440-22C ORCA FLASCH4.0U digital camera. For Notch1 IF combined with ISH of dorsal markers (*wnt11* in cleavage stages, *chordin* in mid-blastula), *Xenopus* pigmented embryos were fixed with MEMPFA for 1 h and cut into right and left halves according to the pigmentation pattern as before. Then, right halves were transferred to Dent's solution, according to the immunodetection protocol, whereas left halves were submitted to the standard ISH protocol. Alternatively, we used albino *Xenopus* embryos to perform Notch1 IF and *wnt11* ISH to correlate their patterns in the same embryo. For this purpose, embryos were fixed in MEMPFA overnight at 4°C and, the following day, they were subjected to the standard ISH protocol. After stringency washings, embryos were washed with TBSE, TBSET and TBSET+BSA as described by Acosta et al. (2011), and were incubated simultaneously with the ISH anti-digoxigenin-AP antibody (Roche, 11093274910, 1/2000) and the IF Notch1 antibody overnight at 4°C. To circumvent the possibility that quenching of IF with the ISH staining could obscure the interpretation of our results, we first proceeded to reveal Notch1 IF and image the embryos as in the standard IF protocol. Then, embryos were individually processed for revealing the *wnt11* ISH in 96× multiwells, and the *wnt11* pattern was correlated with the first image of the same embryo.

Image analysis

Pixel intensity was measured in images of cryosections in regions of interest (ROI) with ImageJ (NIH). For early cleavage stages, we designed a rectangular ROI on the animal hemisphere, and results were plotted as mean pixel intensity (*y*-axis) for each coordinate of the DV axis (*x*-axis) (Fig. 1A′-D′). In addition, two ROIs were selected for each embryo from s1 to s8, one in the dorsal-animal region (dROI) and the other one in the ventral-animal region (vROI). For blastula stages, as the blastocoel cavity precluded the analysis on a rectangular ROI, only comparisons of dROI and vROI were made. For analysis of nuclear IF levels at s8, dorsal and ventral ROIs containing nuclear areas (nROI) were selected, with the DAPI image as a source. Statistical analysis was carried out using Prism (GraphPad) (two-tailed Mann–Whitney *U*-test, $P<0.05$).

Western blot

For WB analysis of Notch1, five whole *Xenopus* embryos (controls, control Mo- or Notch1 Mo-injected embryos) and ten dorsal or ten ventral halves were obtained at the indicated stages in the figures for each round of protein extraction. They were homogenized in 0.15 ml ice-cold PBS containing 1× protease inhibitors (Halt Protease and Phosphatase Inhibitor Cocktail, Thermo Fisher Scientific, 78440). The homogenates were centrifuged for 5 min at 700 ***g*** at 4°C, and the supernatant was precipitated with ten volumes of acetone for 20 min in ice. Samples were centrifuged for 5 min at 3000 ***g*** at 4°C, and the supernatant was discarded. Pellets were dried, then resuspended in 25 µl of 2× Laemmli buffer containing 10% of 2-mercaptoethanol and boiled for 5 min. Then 20 µl of protein samples were separated on an 8% SDS-PAGE gel and transferred to a polyvinylidenedifluoride membrane (Immobilon-P, Millipore, IPVH00010). Blots were blocked in 5% non-fat milk prepared in TTBS (0.05% Tween-20, 10 mM Tris-HCl pH 8, 150 mM NaCl) and then incubated overnight at 4°C with N1 intra Ab, 1/1000 diluted in blocking solution, and with GAPDH monoclonal antibody (6C5) (Thermo Fisher Scientific, AM4300, 1/10,000). After washing three times in TTBS for10 min each, blots were incubated for 2 h at room temperature with HRP-conjugated goat anti-rabbit IgG (H+L) (Jackson ImmunoResearch, 111-035-003, 1/10,000 diluted in blocking solution), and with HRP-conjugated goat anti-mouse IgG (H+L) (Bio-Rad, 1706516, 1/3000). After washing as before, blots were developed in SuperSignal West Pico Chemiluminescent Substrate solution (Thermo Fisher Scientific, 34580) and exposed to film (Agfa-Gevaert). To determine the actual levels of Notch1, the intensity of the bands corresponding to this protein was normalized to the corresponding GAPDH band used as internal control, in each assay.

RT-qPCR methods and primers

For assessing endogenous levels of *notch1* and *wnt11* mRNAs, ventral and dorsal halves of s5 *Xenopus* embryos from two independent batches were cut, according to the pigmentation pattern. For functional experiments, two-cell-stage *Xenopus* embryos from three different batches were injected in both blastomeres with the mRNAs or morpholinos indicated in the figures. The following doses were injected per cell: 1 ng of *nicd1* mRNA, 1 ng of *su(H)1*^{DBM} mRNA, 40 ng of control Mo, 40 ng of Notch1 Mo, or 40 ng of Notch1 Mo+1 ng of *nicd1* mRNA. Embryos were snap frozen at the stages indicated in the figures and stored at −80°C. Ten embryos per biological replicate were used. Total RNAs were purified with an RNeasy kit (Qiagen). Primers are listed in Table S6. New primers were designed using Primer-Blast Software (NCBI). RT reactions were carried out using iScript Reverse Transcription Supermix for RT-qPCR (Bio-Rad). RT-qPCR reactions were performed in triplicate for each sample using SYBRGreen (Thermo Fisher Scientific, K0391) on a CFX qPCR cycler (Bio-Rad, CFX96 C1000 Thermal Cycler, 184-5384). RT-qPCR results were analyzed using Bio-Rad CFX Maestro Software and one-way ANOVA was used to determine statistical significance ($P<0.05$). The relative expression of each target was normalized to *histone4* expression (*H4*).

Gene reporter assay

Two-cell-stage embryos were injected in both blastomeres with 1 pg of circular plasmid pRL-TK (*Renilla* luciferase, Promega, E2231)+40 pg of circular Notch reporter plasmid (4×CSL-firefly luciferase, Addgene, 41726) (Saxena et al., 2001) or with 1 pg of circular plasmid pRL-TK+40 pg of circular Notch reporter plasmid+1 ng of *nicd1* mRNA. Luciferase activity was quantified and normalized to *Renilla* activity in lysates from stage 10.25-10.5 embryos using the Dual-Luciferase Reporter assay system (Promega, E1910) in a TriStar LB 941 Modular Multimode Microplate Reader (Berthold Technologies). For dorsal and ventral luciferase activity quantification, embryos were sectioned in dorsal and ventral halves at stage 10.25-10.5. Five embryos were lysed for each measurement, and ten halves were lysed for each measurement. All assays were performed in duplicate. Embryos from the same fertilization batch were used for each experiment and repeated independently three times. To determine statistical significance, we applied one-way ANOVA analysis and Bonferroni's multiple comparisons test (*t*-test) ($P<0.05$). Statistical analyses were carried out using Prism 6.

Data collection and statistics

Numbers of samples analyzed are indicated for each set of experiments in the figures and supplementary tables. Statistical tests applied are described for each set of experiments in the Materials and Methods sections, in the figures and supplementary tables. Differences were considered significant when $P<0.05$.

Acknowledgements

We acknowledge the following colleagues for providing us with the constructs for making synthetic mRNA and probes: Chris Kintner for *notch1 FL*, *nicd1*, *su(H)1*^{DBM};

Randy Moon for *wnt8a*; Walter Knöchel for *vent-2b*; and Eddy M. de Robertis for *bmp4* and *chordin*. We are also grateful to Andrea Noemí Pecile, Manuel Ponce, Alejo Ramos and Ezequiel Yamus for animal husbandry; to Lucila Morono and Nerina Villalba for technical assistance; to Daniela Rojo and María Belén Favarolo for help with experiments; and to Ana María Adamo, María Cecilia Cirio, and Tomás Falzone for reagents. We are also indebted to Dr Marcelo Rubinstein for his constant support and advice.

Competing interests
The authors declare no competing or financial interests.

Author contributions
Conceptualization: A.M.C.C., S.L.L.; Methodology: A.M.C.C., D.R.R.; Validation: A.M.C.C.; Formal analysis: A.M.C.C., D.R.R., M.V.B., S.L.L.; Investigation: A.M.C.C., D.R.R., P.I.E., M.V.B., R.J.M., M.R.A., L.F.F., S.L.L.; Resources: M.V.B., L.K., L.F.F., S.L.L.; Writing - original draft: S.L.L.; Writing - review & editing: A.M.C.C., D.R.R., M.V.B., L.K., L.F.F., S.L.L.; Visualization: A.M.C.C., D.R.R., M.V.B., S.L.L.; Supervision: S.L.L.; Project administration: S.L.L.; Funding acquisition: S.L.L., L.K., L.F.F.

Funding
Research was supported by the Agencia Nacional de Promoción Científica y Tecnológica, Argentina (PICT 2011-1559 and PICT 2014-2020 to S.L.L.; PICT 2015-1726 and PICT 2016-1429 to L.F.F.; fellowship to R.J.M.), the Consejo Nacional de Investigaciones Científicas y Técnicas, Argentina (PIP 2012-0508 and PIP 2015-0577 to S.L.L.; fellowships to A.M.C.C., D.R.R. and R.J.M.), by the Centre National de la Recherche Scientifique and Aix-Marseille Université, and a research grant from the Fondation pour la Recherche Médicale (DEQ20141231765 to L.K.). M.V.B., L.F.F. and S.L.L. are career researchers of the Consejo Nacional de Investigaciones Científicas y Técnicas. M.V.B. and R.J.M. are researchers-instructors of the Universidad de Buenos Aires.

Supplementary information
Supplementary information available online at
http://dev.biologists.org/lookup/doi/10.1242/dev.159368.supplemental

References
Acosta, H., López, S. L., Revinski, D. R. and Carrasco, A. E. (2011). Notch destabilises maternal beta-catenin and restricts dorsal-anterior development in Xenopus. *Development* **138**, 2567-2579.
Bray, S. and Bernard, F. (2010). Notch targets and their regulation. *Curr. Top. Dev. Biol.* **92**, 253-275.
Chitnis, A., Henrique, D., Lewis, J., Ish-Horowicz, D. and Kintner, C. (1995). Primary neurogenesis in Xenopus embryos regulated by a homologue of the Drosophila neurogenic gene Delta. *Nature* **375**, 761-766.
Christian, J. L. and Moon, R. T. (1993). Interactions between Xwnt-8 and Spemann organizer signaling pathways generate dorsoventral pattern in the embryonic mesoderm of Xenopus. *Genes Dev.* **7**, 13-28.
Cibois, M., Luxardi, G., Chevalier, B., Thomé, V., Mercey, O., Zaragosi, L.-E., Barbry, P., Pasini, A., Marcet, B. and Kodjabachian, L. (2015). BMP signalling controls the construction of vertebrate mucociliary epithelia. *Development* **142**, 2352-2363.
Coffman, C., Harris, W., Kintner, C. (1990). Xotch, the Xenopus homolog of Drosophila notch. *Science* **249**, 1438-1441.
Contakos, S. P., Gaydos, C. M., Pfeil, E. C. and McLaughlin, K. A. (2005). Subdividing the embryo: a role for Notch signaling during germ layer patterning in Xenopus laevis. *Dev. Biol.* **288**, 294-307.
Darken, R. S. and Wilson, P. A. (2001). Axis induction by wnt signaling: target promoter responsiveness regulates competence. *Dev. Biol.* **234**, 42-54.
De Robertis, E. M. (2009). Spemann's organizer and the self-regulation of embryonic fields. *Mech. Dev.* **126**, 925-941.
De Robertis, E. M. and Kuroda, H. (2004). Dorsal-ventral patterning and neural induction in Xenopus embryos. *Annu. Rev. Cell Dev. Biol.* **20**, 285-308.
Efstratiadis, A., Szabolcs, M. and Klinakis, A. (2007). Notch, Myc and breast cancer. *Cell Cycle* **6**, 418-429.
Fainsod, A., Steinbeisser, H. and De Robertis, E. M. (1994). On the function of BMP-4 in patterning the marginal zone of the Xenopus embryo. *EMBO J.* **13**, 5015-5025.
Franco, P. G., Paganelli, A. R., López, S. L. and Carrasco, A. E. (1999). Functional association of retinoic acid and hedgehog signaling in Xenopus primary neurogenesis. *Development* **126**, 4257-4265.
Freeman, S. D., Moore, W. M., Guiral, E. C., Holme, A. D., Turnbull, J. E. and Pownall, M. E. (2008). Extracellular regulation of developmental cell signaling by XtSulf1. *Dev. Biol.* **320**, 436-445.
Gawantka, V., Delius, H., Hirschfeld, K., Blumenstock, C. and Niehrs, C. (1995). Antagonizing the Spemann organizer: role of the homeobox gene Xvent-1. *EMBO J.* **14**, 6268-6279.
Glavic, A., Silva, F., Aybar, M. J., Bastidas, F. and Mayor, R. (2004). Interplay between Notch signaling and the homeoprotein Xiro1 is required for neural crest induction in Xenopus embryos. *Development* **131**, 347-359.
Hawley, S. H., Wünnenberg-Stapleton, K., Hashimoto, C., Laurent, M. N., Watabe, T., Blumberg, B. W. and Cho, K. W. (1995). Disruption of BMP signals in embryonic Xenopus ectoderm leads to direct neural induction. *Genes Dev.* **9**, 2923-2935.
Hayes, J. M., Kim, S. K., Abitua, P. B., Park, T. J., Herrington, E. R., Kitayama, A., Grow, M. W., Ueno, N. and Wallingford, J. B. (2007). Identification of novel ciliogenesis factors using a new in vivo model for mucociliary epithelial development. *Dev. Biol.* **312**, 115-130.
Hayward, P., Brennan, K., Sanders, P., Balayo, T., DasGupta, R., Perrimon, N. and Martinez Arias, A. (2005). Notch modulates Wnt signalling by associating with Armadillo/beta-catenin and regulating its transcriptional activity. *Development* **132**, 1819-1830.
Hayward, P., Kalmar, T. and Martinez Arias, A. (2008). Wnt/Notch signalling and information processing during development. *Development* **135**, 411-424.
Hemmati-Brivanlou, A. and Thomsen, G. H. (1995). Ventral mesodermal patterning in Xenopus embryos: expression patterns and activities of BMP-2 and BMP-4. *Dev. Genet.* **17**, 78-89.
Henningfeld, K. A., Rastegar, S., Adler, G. and Knöchel, W. (2000). Smad1 and Smad4 are components of the bone morphogenetic protein-4 (BMP-4)-induced transcription complex of the Xvent-2B promoter. *J. Biol. Chem.* **275**, 21827-21835.
Hoppler, S. and Moon, R. T. (1998). BMP-2/-4 and Wnt-8 cooperatively pattern the Xenopus mesoderm. *Mech. Dev.* **71**, 119-129.
Ishibashi, H., Matsumura, N., Hanafusa, H., Matsumoto, K., De Robertis, E. M. and Kuroda, H. (2008). Expression of Siamois and Twin in the blastula Chordin/Noggin signaling center is required for brain formation in Xenopus laevis embryos. *Mech. Dev.* **125**, 58-66.
Kamm, G. B., Pisciottano, F., Kliger, R. and Franchini, L. F. (2013). The developmental brain gene NPAS3 contains the largest number of accelerated regulatory sequences in the human genome. *Mol. Biol. Evol.* **30**, 1088-1102.
Kimmel, C. B., Ballard, W. W., Kimmel, S. R., Ullmann, B. and Schilling, T. F. (1995). Stages of embryonic development of the zebrafish. *Dev. Dyn.* **203**, 253-310.
Kirmizitas, A., Meiklejohn, S., Ciau-Uitz, A., Stephenson, R. and Patient, R. (2017). Dissecting BMP signaling input into the gene regulatory networks driving specification of the blood stem cell lineage. *Proc. Natl. Acad. Sci. USA* **114**, 5814-5821.
Klein, S. L. (1987). The first cleavage furrow demarcates the dorsal-ventral axis in Xenopus embryos. *Dev. Biol.* **120**, 299-304.
Kopan, R. and Ilagan, M. X. G. (2009). The canonical Notch signaling pathway: unfolding the activation mechanism. *Cell* **137**, 216-233.
Kuroda, H., Wessely, O. and De Robertis, E. M. (2004). Neural induction in Xenopus: requirement for ectodermal and endomesodermal signals via Chordin, Noggin, beta-Catenin, and Cerberus. *PLoS Biol.* **2**, E92.
Kwon, C., Qian, L., Cheng, P., Nigam, V., Arnold, J. and Srivastava, D. (2009). A regulatory pathway involving Notch1/beta-catenin/Isl1 determines cardiac progenitor cell fate. *Nat. Cell Biol.* **11**, 951-957.
Kwon, C., Cheng, P., King, I. N., Andersen, P., Shenje, L., Nigam, V. and Srivastava, D. (2011). Notch post-translationally regulates β-catenin protein in stem and progenitor cells. *Nat. Cell Biol.* **13**, 1244-1251.
Li, H.-Y., Bourdelas, A., Carron, C., Gomez, C., Boucaut, J.-C. and Shi, D.-L. (2006). FGF8, Wnt8 and Myf5 are target genes of Tbx6 during anteroposterior specification in Xenopus embryo. *Dev. Biol.* **290**, 470-481.
López, S. L., Paganelli, A. R., Siri, M. V. R., Ocaña, O. H., Franco, P. G. and Carrasco, A. E. (2003). Notch activates sonic hedgehog and both are involved in the specification of dorsal midline cell-fates in Xenopus. *Development* **130**, 2225-2238.
Luo, T., Matsuo-Takasaki, M., Thomas, M. L., Weeks, D. L. and Sargent, T. D. (2002). Transcription factor AP-2 is an essential and direct regulator of epidermal development in Xenopus. *Dev. Biol.* **245**, 136-144.
McCrea, P. D., Maher, M. T. and Gottardi, C. J. (2015). Nuclear signaling from cadherin adhesion complexes. *Curr. Top. Dev. Biol.* **112**, 129-196.
McGregor, A. P., Pechmann, M., Schwager, E. E. and Damen, W. G. M. (2009). An ancestral regulatory network for posterior development in arthropods. *Commun. Integr. Biol.* **2**, 174-176.
Muñoz-Descalzo, S., Sanders, P. G. T., Montagne, C., Johnson, R. I., Balayo, T. and Martinez Arias, A. (2010). Wingless modulates the ligand independent traffic of Notch through Dishevelled. *Fly (Austin).* **4**, 182-193.
Muñoz-Descalzo, S., Hadjantonakis, A. and Martinez Arias, A. (2015). Wnt/ß-catenin signalling and the dynamics of fate decisions in early mouse embryos and embryonic stem (ES) cells. *Semin. Cell Dev. Biol.* **47-48**, 101-109.

Nieuwkoop, P. D. and Faber, J. (1994). *Normal Table of Xenopus laevis (Daudin)*. New York and London: Garland Publishing.
Nishimatsu, S., Suzuki, A., Shoda, A., Murakami, K. and Ueno, N. (1992). Genes for bone morphogenetic proteins are differentially transcribed in early amphibian embryos. *Biochem. Biophys. Res. Commun.* **186**, 1487-1495.
Nordin, K. and LaBonne, C. (2014). Sox5 is a DNA-binding cofactor for BMP R-Smads that directs target specificity during patterning of the early ectoderm. *Dev. Cell* **31**, 374-382.
Onichtchouk, D., Gawantka, V., Dosch, R., Delius, H., Hirschfeld, K., Blumenstock, C. and Niehrs, C. (1996). The Xvent-2 homeobox gene is part of the BMP-4 signalling pathway controlling [correction of controling] dorsoventral patterning of Xenopus mesoderm. *Development* **122**, 3045-3053.
Onichtchouk, D., Glinka, A. and Niehrs, C. (1998). Requirement for Xvent-1 and Xvent-2 gene function in dorsoventral patterning of Xenopus mesoderm. *Development* **125**, 1447-1456.
Pizard, A., Haramis, A., Carrasco, A. E., Franco, P., López, S. and Paganelli, A. (2004). Whole-mount in situ hybridization and detection of RNAs in vertebrate embryos and isolated organs. *Curr. Protoc. Mol. Biol.* **66**, 14.9.1-14.9.24.
Popov, I. K., Kwon, T., Crossman, D. K., Crowley, M. R., Wallingford, J. B. and Chang, C. (2017). Identification of new regulators of embryonic patterning and morphogenesis in Xenopus gastrulae by RNA sequencing. *Dev. Biol.* **426**, 429-441.
Ramel, M.-C. and Lekven, A. C. (2004). Repression of the vertebrate organizer by Wnt8 is mediated by Vent and Vox. *Development* **131**, 3991-4000.
Rastegar, S., Friedle, H., Frommer, G. and Knöchel, W. (1999). Transcriptional regulation of Xvent homeobox genes. *Mech. Dev.* **81**, 139-149.
Reversade, B., Kuroda, H., Lee, H., Mays, A. and De Robertis, E. M. (2005). Depletion of Bmp2, Bmp4, Bmp7 and Spemann organizer signals induces massive brain formation in Xenopus embryos. *Development* **132**, 3381-3392.
Revinski, D. R., Paganelli, A. R., Carrasco, A. E. and López, S. L. (2010). Delta-Notch signaling is involved in the segregation of the three germ layers in Xenopus laevis. *Dev. Biol.* **339**, 477-492.
Saka, Y., Tada, M. and Smith, J. C. (2000). A screen for targets of the Xenopus T-box gene Xbra. *Mech. Dev.* **93**, 27-39.
Sakano, D., Kato, A., Parikh, N., McKnight, K., Terry, D., Stefanovic, B. and Kato, Y. (2010). BCL6 canalizes Notch-dependent transcription, excluding Mastermind-like1 from selected target genes during left-right patterning. *Dev. Cell* **18**, 450-462.
Sander, V., Reversade, B. and De Robertis, E. M. (2007). The opposing homeobox genes Goosecoid and Vent1/2 self-regulate Xenopus patterning. *EMBO J.* **26**, 2955-2965.
Sanders, P. G. T., Muñoz-Descalzo, S., Balayo, T., Wirtz-Peitz, F., Hayward, P. and Martinez Arias, A. (2009). Ligand-independent traffic of Notch buffers activated Armadillo in Drosophila. *PLoS Biol.* **7**, e1000169.
Saxena, M. T., Schroeter, E. H., Mumm, J. S. and Kopan, R. (2001). Murine notch homologs (N1-4) undergo presenilin-dependent proteolysis. *J. Biol. Chem.* **276**, 40268-40273.
Scerbo, P., Girardot, F., Vivien, C., Markov, G. V., Luxardi, G., Demeneix, B., Kodjabachian, L. and Coen, L. (2012). Ventx factors function as Nanog-like guardians of developmental potential in Xenopus. *PLoS ONE* **7**, e36855.
Scerbo, P., Marchal, L. and Kodjabachian, L. (2017). Lineage commitment of embryonic cells involves MEK1-dependent clearance of pluripotency regulator Ventx2. *eLife* **6**, e21526.
Schneider, S., Steinbeisser, H., Warga, R. M. and Hausen, P. (1996). Beta-catenin translocation into nuclei demarcates the dorsalizing centers in frog and fish embryos. *Mech. Dev.* **57**, 191-198.
Schohl, A. and Fagotto, F. (2002). Beta-catenin, MAPK and Smad signaling during early Xenopus development. *Development* **129**, 37-52.
Schönauer, A., Paese, C. L. B., Hilbrant, M., Leite, D. J., Schwager, E. E., Feitosa, N. M., Eibner, C., Damen, W. G. M. and McGregor, A. P. (2016). The Wnt and Delta-Notch signalling pathways interact to direct pair-rule gene expression via caudal during segment addition in the spider Parasteatoda tepidariorum. *Development* **143**, 2455-2463.
Session, A. M., Uno, Y., Kwon, T., Chapman, J. A., Toyoda, A., Takahashi, S., Fukui, A., Hikosaka, A., Suzuki, A., Kondo, M. et al. (2016). Genome evolution in the allotetraploid frog Xenopus laevis. *Nature* **538**, 336-343.
Shapira, E., Marom, K., Yelin, R., Levy, A. and Fainsod, A. (1999). A role for the homeobox gene Xvex-1 as part of the BMP-4 ventral signaling pathway. *Mech. Dev.* **86**, 99-111.
Shapira, E., Marom, K., Levy, V., Yelin, R. and Fainsod, A. (2000). The Xvex-1 antimorph reveals the temporal competence for organizer formation and an early role for ventral homeobox genes. *Mech. Dev.* **90**, 77-87.
Smith, W. C. and Harland, R. M. (1991). Injected Xwnt-8 RNA acts early in Xenopus embryos to promote formation of a vegetal dorsalizing center. *Cell* **67**, 753-765.
Sykes, T. G., Rodaway, A. R., Walmsley, M. E. and Patient, R. K. (1998). Suppression of GATA factor activity causes axis duplication in Xenopus. *Development* **125**, 4595-4605.
Tao, Q., Yokota, C., Puck, H., Kofron, M., Birsoy, B., Yan, D., Asashima, M., Wylie, C. C., Lin, X. and Heasman, J. (2005). Maternal wnt11 activates the canonical wnt signaling pathway required for axis formation in Xenopus embryos. *Cell* **120**, 857-871.
Thisse, B. and Thisse, C. (2015). Formation of the vertebrate embryo: moving beyond the Spemann organizer. *Semin. Cell Dev. Biol.* **42**, 94-102.
Wessely, O., Agius, E., Oelgeschläger, M., Pera, E. M. and De Robertis, E. M. (2001). Neural induction in the absence of mesoderm: beta-catenin-dependent expression of secreted BMP antagonists at the blastula stage in Xenopus. *Dev. Biol.* **234**, 161-173.
Wettstein, D. A., Turner, D. L. and Kintner, C. (1997). The Xenopus homolog of Drosophila suppressor of hairless mediates Notch signaling during primary neurogenesis. *Development* **124**, 693-702.
Yan, B., Neilson, K. M. and Moody, S. A. (2009). foxD5 plays a critical upstream role in regulating neural ectodermal fate and the onset of neural differentiation. *Dev. Biol.* **329**, 80-95.

Supplementary Material for Castro Colabianchi et al. (2018)

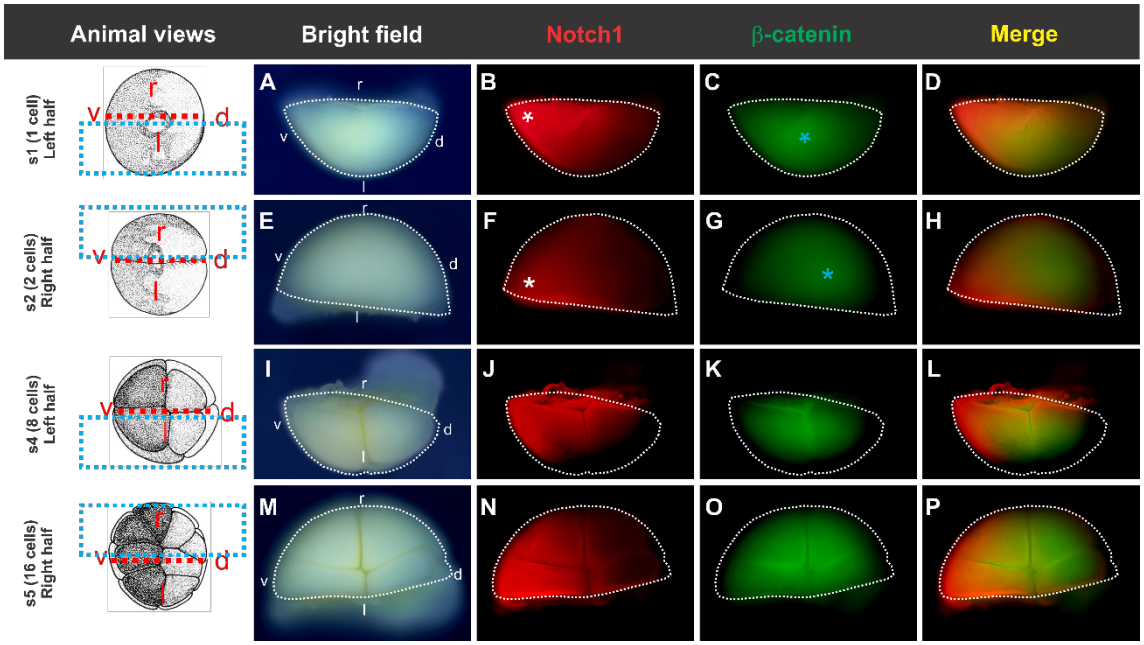

Figure. S1. Distribution of endogenous Notch 1 and β-catenin proteins from s1 through cleavage stages in *Xenopus* embryos (animal views). Left and right halves of embryos were cut at the indicated Nieuwkoop and Faber stages (s) (left column, turquoise dotted boxes) and processed for whole-mount IF. The embryonic early axes were predicted according to the original pigmentation. (A,E,I,M) Bright field views. (B,F,J,N) Notch1 IF. (C,G,K,O) Total β-catenin IF. (D,H,L,P) Merged images of Notch1 and total β-catenin IF. We noted that in some early embryos, the highest levels of total β-catenin IF located relatively more dorsally (light blue asterisks) than the region were the highest levels of Notch1 IF were found (white asterisks) (see Table S2). d, dorsal; v, ventral; l, left; r, right.

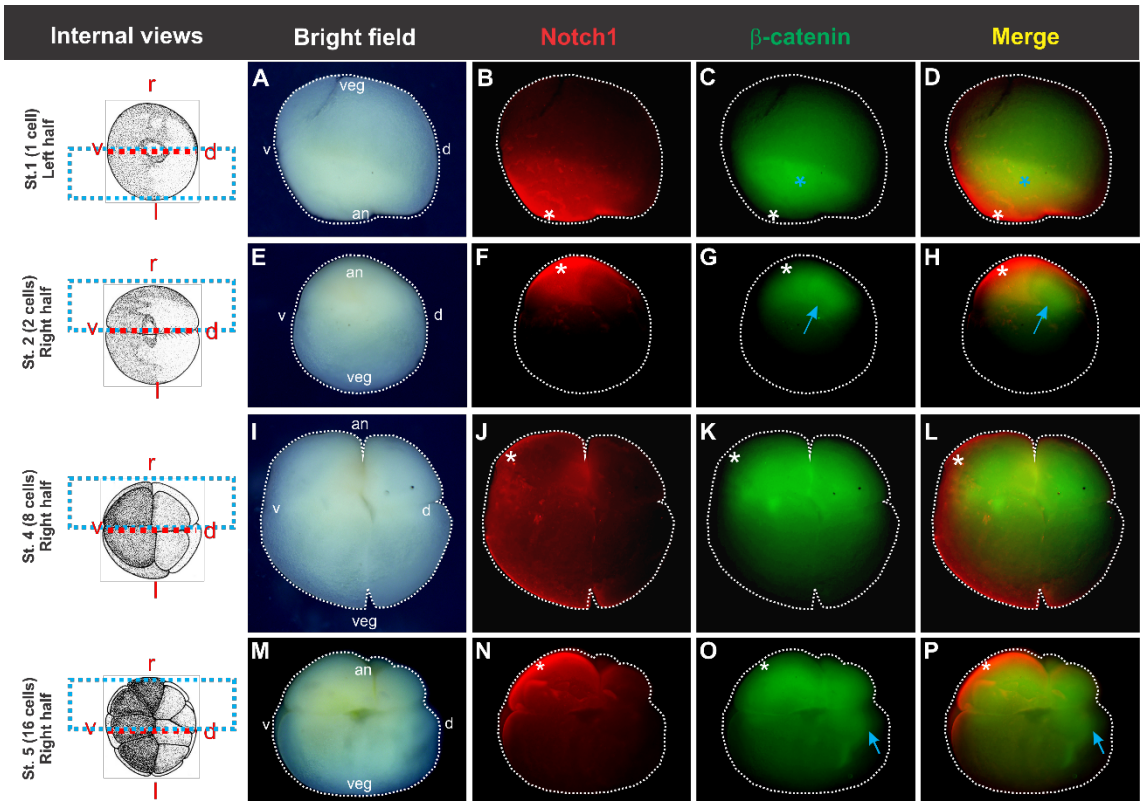

Figure S2. Distribution of endogenous Notch 1 and β-catenin proteins from s1 through cleavage stages in *Xenopus* embryos (internal views). Left and right halves of embryos that were cut at the indicated Nieuwkoop and Faber stages (s) (left column, turquoise dotted boxes) and processed for whole-mount IF. The embryonic early axes were predicted according to the original pigmentation. (A,E,I,M) Bright field views. (B,F,J,N) Notch1 IF. (C,G,K,O) Total β-catenin IF. (D,H,L,P) Merged images of Notch1 and total β-catenin IF. We noted that in some whole-mount halves from early embryos, total β-catenin IF appeared to have a dorsal bias (light blue arrows) or its highest levels were apparently in a different place (light blue asterisk) in relation to the region were the strongest Notch1 IF was found (white asterisks) (See Table S2). d, dorsal; v, ventral; l, left; r, right; an, animal; veg, vegetal.

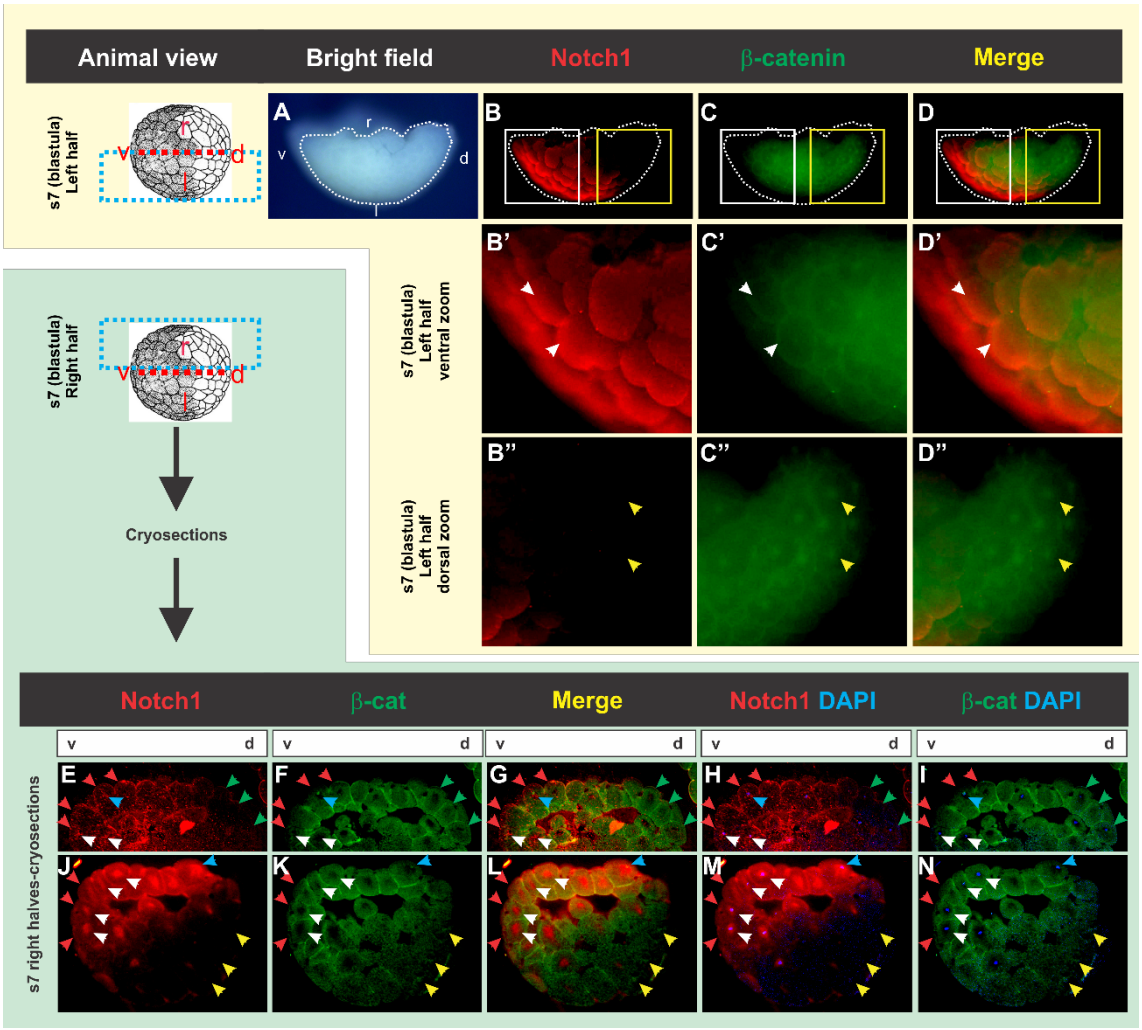

Figure. S3. Distribution of endogenous Notch 1 and β-catenin proteins at s7 in *Xenopus* embryos. Left and right halves of embryos were cut at the indicated Nieuwkoop and Faber stages (s) (left column, turquoise dotted boxes) and processed for whole-mount IF (A-D'') or for IF in cryosections (E-N). The embryonic early axes were predicted according to the original pigmentation. (A) Bright field view. (B-B'',E,J) Notch1 IF. (C-C'',F,K) Total β-catenin IF. (D-D'',G,L), merged images of Notch1 and total β-catenin IF. (B'-D') Higher magnifications of the ventral region depicted by the white boxes in B-D. (B''-D'') Higher magnifications of the dorsal region depicted by the yellow boxes in B-D. Cells in the ventral-most side, with the highest Notch1 IF (white arrows, B',D') stained weaker for nuclear β-catenin (white arrows, C') in comparison with cells of the dorsal side (yellow arrows, C'',D''), which have the lowest Notch1 IF (yellow arrows, B''). (E, J) According to the DV orientation assigned by pigment distribution, Notch1 was significantly enriched in the ventral region in cryosections (8/9 embryos, $P<0.0001$; Mann-Whitney test; table S1). The pattern of total β-catenin is complex (F,G,I,K,L,N), with membrane-associated and cytoplasmic pools and some immunopositive nuclei

(yellow arrows) that begin to be detected at this stage. We found embryos with a significant dorsal enrichment of total β-catenin (F) (4/9 embryos) and others with more ventral staining (K), according to pigment distribution (P<0.0001; Mann-Whitney test; see Table S1), although nuclear β-catenin begins to be detected in some dorsal nuclei (yellow arrows). One of the 9 embryos at s7 (Table S1) showed dorsal Notch1 enrichment and ventral total β-catenin enrichment, and this might be due to the inaccurate DV orientation assigned by pigment distribution; thus, this would render another embryo with ventral Notch1 and dorsal β-catenin. Notch1 is detected in ventral nuclei, which do not show strong nuclear β-catenin staining (white arrows), although some nuclei stain for both proteins (turquoise arrows). Note the lower total β-catenin IF in the apical region of the ventral-most cells, which shows instead high Notch1 IF (red arrows), consistent with the pattern in the whole-mount views, whereas in the embryo with dorsal β-catenin enrichment in E-I, there is higher β-catenin IF in the apical region of the dorsal cells (green arrows). d, dorsal; v, ventral; l, left; r, right.

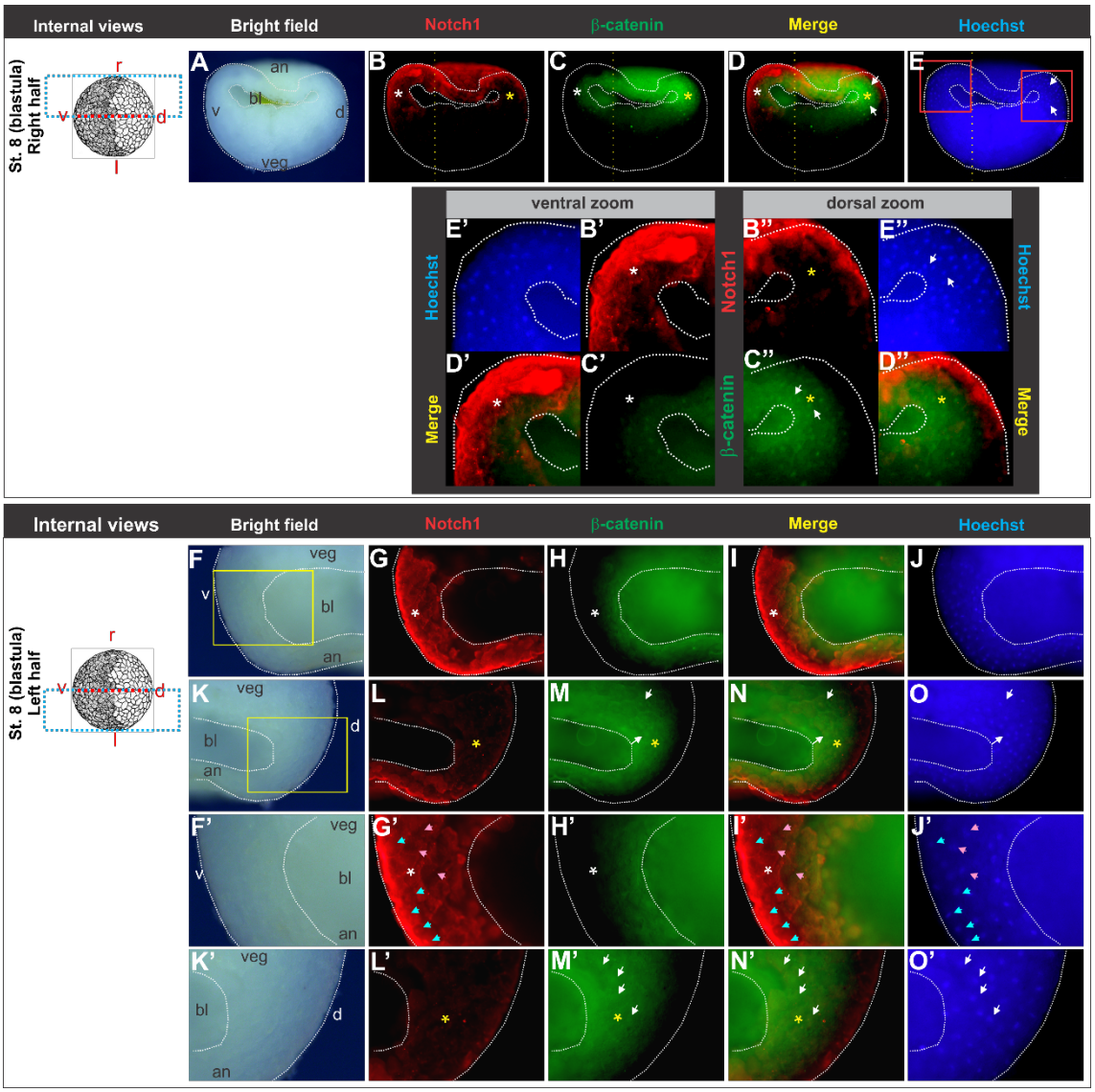

Figure. S4. Distribution of endogenous Notch 1 and β-catenin proteins in *Xenopus* mid blastula (internal views). Internal views of right (A-D'') and left (F-O´) halves of embryos that were cut at s8 (as shown in the left column, turquoise dotted boxes) and processed for whole-mount IF. The embryonic early axes were predicted according to the original pigmentation. (A,F,F',K,K') Bright field views. (B-B'',G,G',L,L') Notch1 IF. (C-C'',H,H',M,M') Total β-catenin IF. (D-D'',I,I',N,N') Merged images of Notch1 and total β-catenin IF. (E-E'',J,J',O,O') Nuclear Hoechst staining. The vertical yellow dotted lines in (B-E) indicate the photocomposition of images taken at two slightly different focal planes to keep nuclei in focus in the dorsal and ventral region of the embryo. (B'-E') Higher magnification of the ventral region of the images shown in B-E, corresponding to the area indicated by the left red box in E. (B''-E'') Higher magnification of the dorsal region of the images shown in B-E, corresponding to the area indicated by the right red

box in E. (F-J) and (K-O) Ventral and dorsal regions, respectively, of the same embryo. (F'-J') and (K'-O') Higher magnifications of F-J and K-O, respectively, corresponding to the yellow boxed area in F and K. Notch1 protein is more enriched in the ventral (white asterisks) than in the dorsal region (yellow asterisks) whereas the opposite occurs with nuclear β-catenin (white arrows). These patterns were consistently found both in right and left halves at this stage in embryos from different batches (94%, n=18, 3 batches of embryos; see Table S2). Interestingly, amongst the ventral cells, we could distinguish Notch1^{+} nuclei in several cells (G',I',J', light blue arrows) while others did not appear to have nuclear Notch1 accumulation (G',I',J', pink arrows). Bl, blastocoel cavity; d, dorsal; v, ventral; l, left; r, right; an, animal; veg, vegetal.

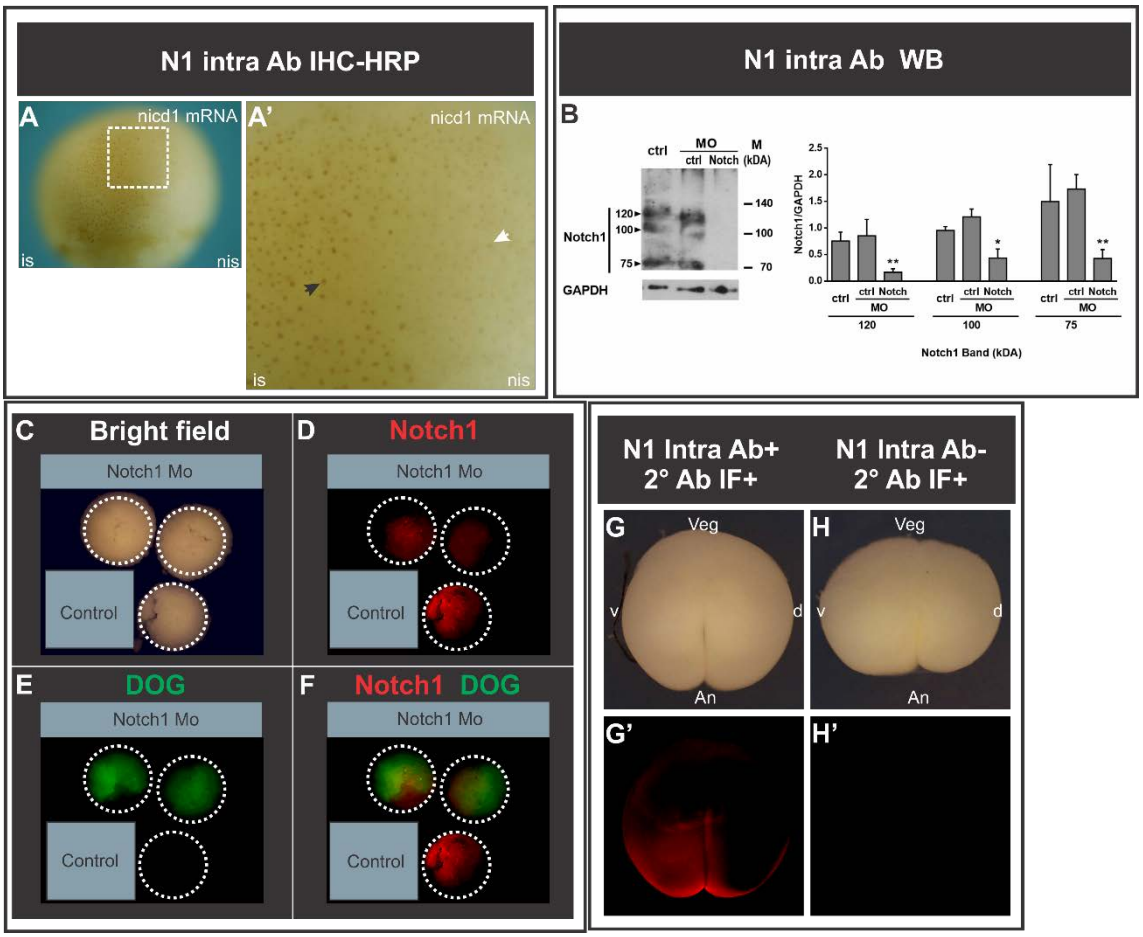

Figure S5. Notch1 intra antibody ab8387 (N1 intra Ab) specifically recognizes Notch1 protein in *Xenopus laevis* embryos. (A,A') Embryo unilaterally injected with 1 ng of *Xenopus laevis nicd1* mRNA into 1 cell at the 2-cells stage, fixed at gastrula stage and processed for immunohistochemistry with a horseradish peroxidase-conjugated secondary antibody (IHC-HRP). (A') Higher magnification view of the area indicated by the dashed box in A. Diaminobenzidine brown development clearly showed a very strong and dense nuclear staining (black arrow) on the injected side (is), confirming that N1 intra Ab recognizes *Xenopus laevis* NICD1 when overexpressed. The non-injected side (nis) showed a lighter staining in scattered nuclei (white arrow), indicating that N1 intra Ab could also detect the endogenous NICD1. (B) Western blot (WB) analysis of protein extracts obtained at s15 from uninjected controls (ctrl), embryos injected with 80 ng of Control Mo (ctrl MO) or with 80 ng of Notch1 Mo (Notch MO) at the 1-cell stage. The N1 intra Ab recognizes bands corresponding to Notch1 normal processing (Kopan and Ilagan, 2009) in extracts from uninjected controls and from Control MO-injected embryos: one around 120 kDa, which is expected to correspond to the Notch1 fragments containing the transmembrane domain (Notch transmembrane and intracellular domain, NTMIC; Notch extracellular truncation, NEXT) and a band of around 100 kDa, which is expected to correspond to NICD (Notch intracellular domain), as has been previously

shown with other antibodies recognizing Notch1 in cell and embryo extracts from mammals (Zagouras et al., 1995) (Blaumueller et al., 1997) (De Falco et al., 2015). A lower molecular weight band of 75 kDa was also observed at this stage. The three bands are specific, since they were significantly reduced by Notch1 Mo (* $P< 0.05$, ** $P< 0.01$, One Way ANOVA test). Results are shown as the mean+s.e.m. of three independent experiments. (C-F) N1 intra Ab IF (D,F, red channel) in animal hemispheres from s6 embryos that were injected at s1 with 60 ng of Notch1 Mo + DOG as tracer (upper embryos) and from a sibling uninjected control (lower embryo), photographed together. (C) Bright field image. (E, F) Green fluorescence from the tracer. Notch1 Mo decreased N1 intra Ab IF in all injected embryos (n=10), confirming that N1 intra Ab specifically recognizes Notch1 protein in *Xenopus* embryos. (G-H') Internal views of left halves of 4-cells embryos processed for IF with anti-rabbit IgG-Alexa 594 as secondary antibody (2° Ab), with (G,G') or without (H,H') N1 intra Ab primary antibody. (G,H) Bright field. (G´,H') Fluorescence image, red channel, of the same embryos shown in G,H, respectively. The secondary antibody did not show non-specific fluorescence. d, dorsal; v, ventral; An, animal; Veg, vegetal.

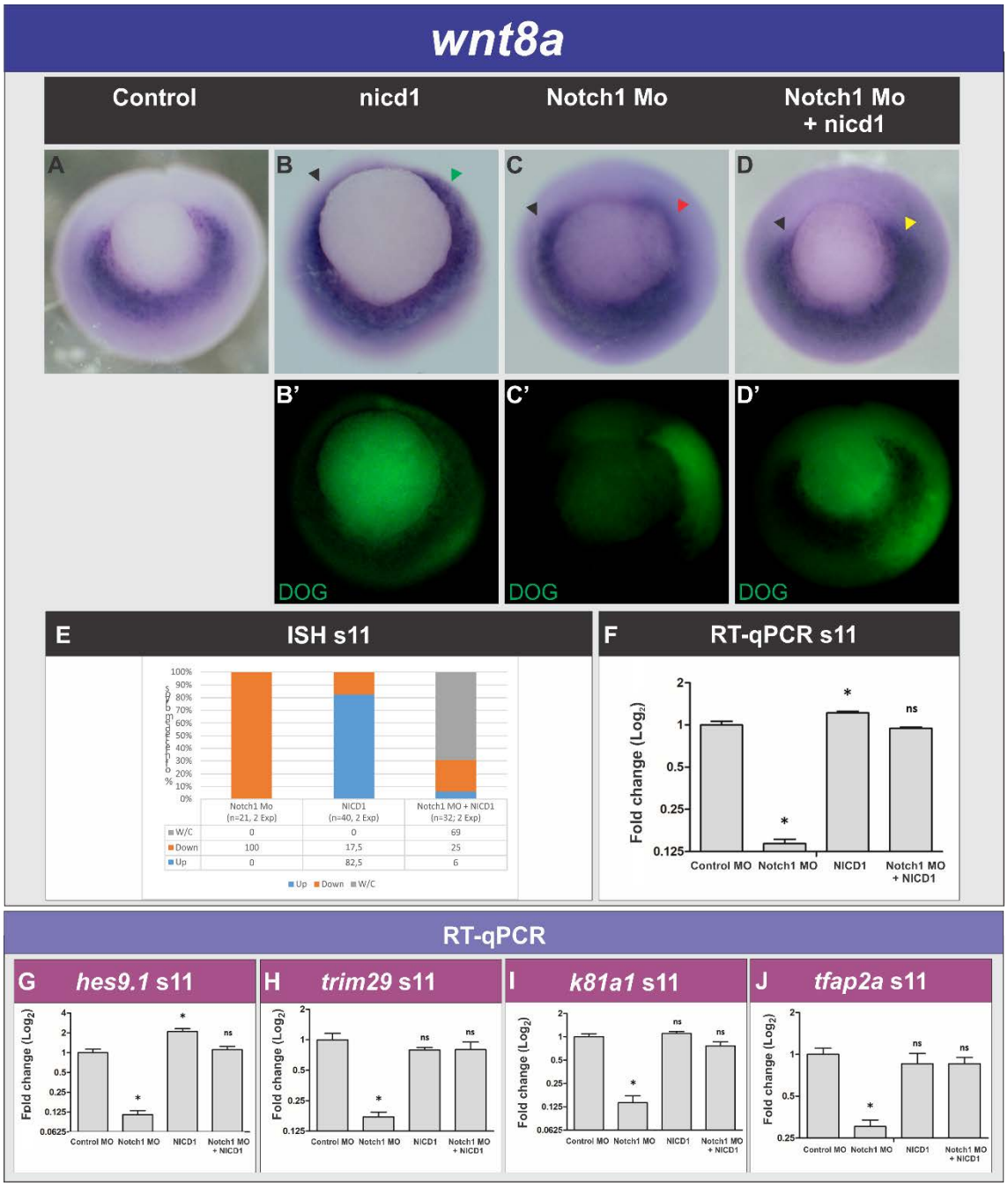

Figure S6. Rescue experiments showing the specificity of Notch1 Mo and that *notch1* is necessary for the expression of other genes of the ventral program.

(A) Uninjected control. (B-D) Embryos unilaterally injected at the 2-cells stage with 1 ng of *nicd1 mRNA* (B), 40 ng of Notch1 Mo (C), or with 40 ng of Notch1 Mo + 1 ng of *nicd1* mRNA (D). (B'-D') Fluorescence of the co-injected tracer DOG. The effect of the injections was assessed by comparing the expression pattern of *wnt8a* in the injected side (shown at the right side of the photographs) with the non-injected side (black arrowheads, B-D). *nicd1* expanded *wnt8a* expression in the injected side in the dorsal

region (compare green and black arrowheads). The down-regulation of *wnt8a* in the injected side by Notch1 Mo (red arrowhead, C) was rescued by co-injection of *nicd1* mRNA (yellow arrowhead, D). (E) Summary of the rescue results analyzed by ISH, expressed as the percentage of embryos showing the changes in *wnt8a* expression indicated by the color codes. Cyan, up-regulated; orange, down-regulated; gray, without changes (w/c). The number of total embryos analyzed (n) and the number of independent experiments (Exp) are indicated below the bars. (F-J) RT-qPCR quantification at s11 of the following mRNAs: *wnt8a* (F), the *bonafide* Notch target *hes9.1* (G), and the ventral markers *trim29* (H), *k81a1* (I), and *tfap2a* (J). Notch1 Mo significantly down-regulated all of these genes, whereas *nicd1* mRNA completely rescued their down-regulation produced by Notch1 Mo. Results are represented as the mean+s.e.m. Statistical significant differences between means in relation to the Control Mo injection are indicated with asterisks (P<0.05; One-way ANOVA analysis). Nieuwkoop and Faber stages (s) are indicated in each panel.

Stage	Notch1 V>D	Notch1 D>V	Total β-cat D>V	Total β-cat V>D	Total β-cat V=D	Nuc β–cat D>V	Nuc Notch1 V>D	n
1-2	9	4	6	5	2	N.A.	N.A.	13
3	3	0	0	3	0	N.A.	N.A.	3
4	1	0	0	1	0	N.A.	N.A.	1
7	8	1	4	5	0	N.A.	N.A.	9
8	2	0	2	0	0	**2**	**2**	**2**
TOTAL (s1-s8)	**23**	**5**	**12**	**14**	**2**			**28**

Stage	Notch1 V>D %	Notch1 D>V %	Total β-cat D>V %	Total β-cat V>D %	Total β-cat V=D %	Nuc β–cat D>V (%)	Nuc Notch1 V>D (%)	n
1-2	69%	31%	46%	38%	15%	N.A.	N.A.	13
3	100%	0%	0%	100%	0%	N.A.	N.A.	3
4	100%	0%	0%	100%	0%	N.A.	N.A.	1
7	89%	11%	44%	56%	0%	N.A.	N.A.	9
8	100%	0%	100%	0%	0%	**100%**	**100%**	**2**
TOTAL (s1-s8)	**81%**	**19%**	**41%**	**52%**	**7%**			**28**

Table S1. Distribution of Notch1 and β-catenin IF in cryosections of *Xenopus* embryos after quantification of intensity levels with Image J. Analysis: two-tailed Mann-Whitney test (P<0.05) (dROI vs. vROI). N.A., not analyzed. The upper part shows results expressed as absolute numbers of embryos. The lower part shows results expressed as percentage of embryos analyzed.

Stage	Half	Total βcat/N1 D>V	Nuc βcat D>V	Max βcat displaced from Max N1 (*)	n (per half)	n (per stage)	%
1	LEFT	3	N.A.	3	3	5	
1	RIGHT	2	N.A.	2	2		
2	LEFT	1	N.A.	1	2	3	
2	RIGHT	2	N.A.	1	1		
3	LEFT	1	N.A.	1	1	7	
3	RIGHT	6	N.A.	1	6		
4	LEFT	1	N.A.	0	2	3	
4	RIGHT	2	N.A.	0	1		
5	RIGHT	1	N.A.	1	1	1	
6	RIGHT	2	N.A.	N.A.	2	2	
6.5	LEFT	2	N.A.	N.A.	2	4	
6.5	RIGHT	2	N.A.	N.A.	2		
7-7.5	LEFT	3	N.A.	N.A.	3	7	
7-7.5	RIGHT	4	N.A.	N.A.	4		
8	LEFT	8	8	N.A.	10	18	
8	RIGHT	10	9	N.A.	8		
	TOTAL	50	17		50		
% βcat/N1 D>V (s1-s8)	**50**				**50**		**100%**
% nuc βcat D>V (s8)	**17**				**18**		**94%**
% Max βcat displaced from Max N1 (S1-S5)	**10**				**19**		**53%**

Table S2. Qualitative analysis of β-catenin (βcat) IF distribution in whole-mount left and right halves was restricted to hemi-dissected embryos which showed ventrally located Notch1 (N1). Images showed that β-catenin IF (green fluorescence) prevailed over Notch1 IF (red fluorescence) in the dorsal region (total βcat/N1 column), as shown in the examples of merged images presented throughout Fig. S1-S4. For this analysis, embryos were collected from three independent batches. N.A., not analyzed. (*) Although we were not able to distinguish a clear dorsal bias of total β-catenin at early cleavage stages by this analysis, the maximum level of β-catenin IF (Max βcat) occasionally seemed to be displaced from the zone of highest level of Notch1 IF (Max N1) in the ventral side (53% of embryos from s1 to s5, n=19). This analysis was made only in embryos with few cells, as the total β-catenin pattern is more complex when cellularization increases.

Stage	Notch1 opposite to *wnt11*	Notch1 opposite to *chrd*	Notch1 opposite to both dorsal markers	n	%	Method
s1-s6	11			11		Left (*wnt11* ISH) and right (Notch1 IF) contralateral halves from pigmented embryos, processed in separate pools for each marker
s1-s6	7			8		Individually processed albino embryos, followed sequentially (1st Notch1 IF, 2nd *wnt11* ISH)
s8		4		4		Left (*chrd* ISH) and right (Notch1 IF) contralateral halves from pigmented embryos, processed in separate pools for each marker
TOTAL s1-s6 (opposite to *wnt11*)	18			19	95%	
TOTAL s8 (opposite to *chrd*)		4		4	100%	
TOTAL s1-s8 (opposite to *wnt11* + *chrd*)			22	23	96%	

Table S3-A. Distribution of Notch1 (IF) and dorsal markers *wnt11* (s1 to s6, ISH) and *chordin (chrd)* (s8, ISH) in *Xenopus* embryos, grouped by method of analysis.

Stage	Notch1 opposite to *wnt11*	Notch1 opposite to *chrd*	Notch1 symmetric	Notch1 opposite to both dorsal markers	n	% Notch1 opposite to dorsal marker
s1	6		0		6	100%
s2	3		0		3	100%
s3	2		0		2	100%
s4	1		1		2	50%
s5-s6	6		0		6	100%
s8		4	0		4	100%
TOTAL s1-s6 (opposite to *wnt11*)	18		1		19	95%
TOTAL s8 (opposite to *chrd*)		4	0		4	100%
TOTAL s1-s8 (opposite to *wnt11* + *chrd*)			1	22	23	96%

Table S3-B. Distribution of Notch1 (IF) and dorsal markers *wnt11* (s1 to s6, ISH) and *chordin (chrd)* (s8, ISH) in *Xenopus* embryos at the indicated stages (s).

Stage	Notch1 IF opposite to β-catenin IF	n	%
1 cell	4	4	100%
2 cells	8	9	89%
4 cells	12	14	86%
8 cells	6	7	86%
32+ cells/blastula	13	15	87%
TOTAL	**43**	**49**	**88%**

Table S4. Qualitative analysis of Notch1 IF distribution in relation to β-catenin IF distribution in whole-mount zebrafish embryos.

Stage	*notch1* mRNA V>D	*notch1* mRNA V<D	*notch1* mRNA V=D	n	*notch1* mRNA V>D (%)
s1	5	0	0	5	100%
s2	9	0	0	9	100%
s3	6	0	0	6	100%
s4	6	1	0	7	86%
s5	4	0	0	4	100%
s6	4	1	0	5	80%
s7	5	0	0	5	100%
s8	15	5	1	21	71%
TOTAL	**54**	**7**	**1**	**62**	**87%**

Table S5. Analysis of *notch1* mRNA distribution by ISH in left halves of *Xenopus* embryos. The DV axis was assigned by pigment distribution. Summary of three independent batches of embryos.

Primers	Origin	Sequence
tfap2a	(Morgan et al., 2004)	U: 5’-TCC CAA CAG CCA TAC AGA CA-3’ D: 5’-AGT TGG TGG CTG CAG AAA GT-3’
bmp4	(Xanthos et al., 2002)	U: 5'-ACC CAT AGC TGC AAA TGG AC-3' D: 5'-CAT GCT TCC CCT GAT GAG TT-3'
H4	(Cao et al., 2007)	U: 5'-GGC AAA GGA GGA AAA GGA CTG-3' D: 5'-GGT GAT GCC CTG GAT GTT GT 3'
hes9.1	New	U:5'-GCT TCC AAA TAT GCA CAA TCA TCC-3' D:5'-CCA GTC CCA GGA GTT GTG CAT TT-3'
k81a1	(de Crozé et al., 2011)	U: 5'-CAC CAG AAC ACA GAG TAC-3' D: 5'-CAA CCT TCC CAT CAA CCA-3'
notch1	New	U:5'-CCG TGC AAA AAT GGA GCC AA-3' D:5'-GCC CGG TGA AAC CTT CTG T-3'
trim29	(Castillo-Briceno and Kodjabachian, 2014)	U: 5’-TGG AAA TCA GCT AAG CCG ACC CT-3’ D: 5’-TGC CCT GCT GCC ATA ATC TGT CA-3’
vent-2b	New	U:5'-AGA CGT AAA CTC GCA GCC AA-3' D:5'-GCT GGG TGG TAT GAG TCT GG-3'
ventx2.1	(Kofron et al., 2004)	U: 5'-CCT CTG TTG AAT GGC TTG CT-3' D: 5'-TGA GAC TTG GGC ACT GTC TG-3'
wnt11	(Tao et al., 2005)	U: 5’-TGA CAG CTG CAA CCT CAT GT-3’ D: 5’-ACA GAG GGC TGT CAG TGC TT-3’
wnt8a	(Xanthos et al., 2002)	U: 5'-CTG ATG CCT TCA GTT CTG TGG-3' D: 5'-CTA CCT GTT TGC ATT GCT CGC-3'

Table S6. Primer pairs for RT-qPCR.

Supplementary references

Blaumueller, C. M., Qi, H., Zagouras, P. and Artavanis-Tsakonas, S. (1997). Intracellular Cleavage of Notch Leads to a Heterodimeric Receptor on the Plasma Membrane. *Cell* **90**, 281–291.

Cao, Y., Siegel, D., Donow, C., Knöchel, S., Yuan, L. and Knöchel, W. (2007). POU-V factors antagonize maternal VegT activity and beta-Catenin signaling in Xenopus embryos. *EMBO J.* **26**, 2942–54.

Castillo-Briceno, P. and Kodjabachian, L. (2014). Xenopus embryonic epidermis as a mucociliary cellular ecosystem to assess the effect of sex hormones in a non-reproductive context. *Front. Zool.*

de Crozé, N., Maczkowiak, F. and Monsoro-Burq, A. H. (2011). Reiterative AP2a activity controls sequential steps in the neural crest gene regulatory network. *Proc. Natl. Acad. Sci. U. S. A.* **108**, 155–60.

De Falco, F., Sabatini, R., Papa, B. Del, Falzetti, F., Ianni, M. Di, Sportoletti, P., Baldoni, S., Screpanti, I., Marconi, P. and Rosati, E. (2015). Notch signaling sustains the expression of Mcl-1 and the activity of eIF4E to promote cell survival in CLL. *Oncotarget* **6**,.

Kofron, M., Puck, H., Standley, H., Wylie, C., Old, R., Whitman, M. and Heasman, J. (2004). New roles for FoxH1 in patterning the early embryo. *Development* **131**, 5065–78.

Kopan, R. and Ilagan, M. X. G. (2009). The canonical Notch signaling pathway: unfolding the activation mechanism. *Cell* **137**, 216–233.

Morgan, M. J., Woltering, J. M., In der Rieden, P. M. J., Durston, A. J. and Thiery, J. P. (2004). YY1 regulates the neural crest-associated slug gene in Xenopus laevis. *J. Biol. Chem.* **279**, 46826–34.

Tao, Q., Yokota, C., Puck, H., Kofron, M., Birsoy, B., Yan, D., Asashima, M., Wylie, C. C., Lin, X. and Heasman, J. (2005). Maternal wnt11 activates the canonical wnt signaling pathway required for axis formation in Xenopus embryos. *Cell* **120**, 857–871.

Xanthos, J. B., Kofron, M., Tao, Q., Schaible, K., Wylie, C. and Heasman, J. (2002). The roles of three signaling pathways in the formation and function of the Spemann Organizer. *Development* **129**, 4027–4043.

Zagouras, P., Stifani, S., Blaumueller, C. M., Carcangiu, M. L. and Artavanis-Tsakonas, S. (1995). Alterations in Notch signaling in neoplastic lesions of the human cervix. *Proc. Natl. Acad. Sci. U. S. A.* **92**, 6414–8.